ISTITUTO DI ANALISI DEI SISTEMI ED INFORMATICA
"Antonio Ruberti"
CONSIGLIO NAZIONALE DELLE RICERCHE

A. Bertuzzi, A. Fasano, A. Gandolfi, C. Sinisgalli

MODELLING THE EVOLUTION OF A TUMOURAL MULTICELLULAR SPHEROID AS A TWO-FLUID BINGHAM-LIKE SYSTEM

R. 9, 2012

Alessandro Bertuzzi – Istituto di Analisi dei Sistemi ed Informatica "A. Ruberti", CNR, Viale Manzoni 30, 00185 Roma, Italy. `alessandro.bertuzzi@iasi.cnr.it`.

Antonio Fasano – Dipartimento di Matematica "U. Dini", Università di Firenze, Viale Morgagni 67/A, 50134 Firenze, Italy. `fasano@math.unifi.it`.

Alberto Gandolfi – Istituto di Analisi dei Sistemi ed Informatica "A. Ruberti", CNR, Viale Manzoni 30, 00185 Roma, Italy. `alberto.gandolfi@iasi.cnr.it`.

Carmela Sinisgalli – Istituto di Analisi dei Sistemi ed Informatica "A. Ruberti", CNR, Viale Manzoni 30, 00185 Roma, Italy. `carmela.sinisgalli@iasi.cnr.it`.

ISSN: 1128–3378

Collana dei Rapporti dell'Istituto di Analisi dei Sistemi ed Informatica "Antonio Ruberti", CNR

viale Manzoni 30, 00185 ROMA, Italy

tel. ++39-06-77161
fax ++39-06-7716461
email: `iasi@iasi.cnr.it`
URL: `http://www.iasi.cnr.it`

Abstract

In this paper we propose a model for the evolution of a tumour spheroid assuming a structure in which the central necrotic region contains an inner liquid core surrounded by dead cells that keep some mechanical integrity. This partition is a consequence of assuming that a finite delay is required for the degradation of dead cells into liquid. The phenomenological assumption of constant local volume fraction of cells is also made. The above structure is coupled with a mechanical two-phase model that views the cell component as a Bingham-like fluid and the extracellular liquid as an inviscid fluid. By imposing the continuity of the normal stress throughout the whole spheroid, we can describe the spheroid evolution and characterize the possible steady state. Depending on the values of mechanical parameters, the model predicts either an evolution toward the steady state or an unbounded growth. An existence and uniqueness result has been proved under suitable assumptions, along with some qualitative properties of the solution.

Modelling the evolution of a tumoural multicellular spheroid as a two-fluid Bingham-like system

Alessandro Bertuzzi[1], Antonio Fasano[1,2], Alberto Gandolfi[1], Carmela Sinisgalli[1]

[1]Istituto di Analisi dei Sistemi ed Informatica “A. Ruberti” - CNR
Viale Manzoni 30, 00185 Roma, Italy
e-mail: alessandro.bertuzzi@iasi.cnr.it, alberto.gandolfi@iasi.cnr.it, carmela.sinisgalli@iasi.cnr.it

[2]Dipartimento di Matematica “U. Dini”, Universita’ di Firenze
Viale Morgagni 67/A, 50134 Firenze, Italy
e-mail: fasano@math.unifi.it

Abstract

In this paper we propose a model for the evolution of a tumour spheroid assuming a structure in which the central necrotic region contains an inner liquid core surrounded by dead cells that keep some mechanical integrity. This partition is a consequence of assuming that a finite delay is required for the degradation of dead cells into liquid. The phenomenological assumption of constant local volume fraction of cells is also made. The above structure is coupled with a mechanical two-phase model that views the cell component as a Bingham-like fluid and the extracellular liquid as an inviscid fluid. By imposing the continuity of the normal stress throughout the whole spheroid, we can describe the spheroid evolution and characterize the possible steady state. Depending on the values of mechanical parameters, the model predicts either an evolution toward the steady state or an unbounded growth. An existence and uniqueness result has been proved under suitable assumptions, along with some qualitative properties of the solution.

1 Introduction

Cells from different tumour cell lines can be grown *in vitro* to form spheroidal masses, called multicellular tumour spheroids, currently considered valuable experimental models of avascular tumours [46, 36, 29, 37]. Multicellular tumour spheroids have been, and are, the object of comprehensive investigations since they provide a useful model to assess the effects of oxygenation, nutrition and external mechanical actions on tumour growth, as well as the effects of anticancer treatments with drugs and radiation.

During the spheroid growth the fraction of proliferating cells decreases, and when cells in the inner region become deprived of oxygen, glucose and other nutrients, and/or metabolic waste accumulates, cell death occurs. Thus, in a late growth stage, the spheroids consist of an outer viable rim (whose thickness takes values in the typical range $100 \div 250 \mu$m) surrounding a central necrotic region. The spheroid growth is initially exponential and then it tends to saturate. Examples of spheroids reaching the stationary state (with final diameter of $1 \div 3$ mm) have been reported [24, 26].

Multicellular spheroids have been studied quite extensively under different viewpoints and adopting different modelling approaches (for a review see [3, 6, 34]). The so-called two-fluid scheme, in which not only extracellular fluid, but also the cell aggregate is treated as a fluid, has been used quite frequently because of its simplicity [14, 16, 17]. In that framework the seemingly simple problem of predicting the size of a stationary spheroid has been reconsidered in [23] and in [20, 21], with the aim of formulating a model keeping most of the physics but involving just a small number of parameters (see [22] for an extended discussion). In [23] a heuristic argument based on energy balance was introduced, while in [20] a more rigorous approach was pursued, based on a finer stress analysis. Here we want to describe the evolution of the spheroid from some initial non-necrotic stage, basically in the same framework as [20], though with some nontrivial changes. The main novelty is that the cells aggregate is represented as a Bingham fluid. Such a choice makes the two-fluid scheme much more realistic, since the yield stress characterizing the Bingham fluid mimics reasonably well the nature of cell-cell adhesion forces, exerted by bonds having a rupture threshold. It is not surprising that in the new mechanical framework the scheme becomes considerably more complicated. We will illustrate how the present paper relates to the previous literature including similar effects during the model development. At the same time we will point out both the original aspects and the limitations of the model.

The outline of the paper is the following. Modelling assumptions are discussed in Section 2, in which the partition of necrotic region in a liquid core surrounded by a "solid" shell is introduced, and the Bingham model for the cell aggregate is presented in Section 3. Section 4 describes the partition of the spheroid into proliferating, quiescent and necrotic regions by level sets of the oxygen concentration. The fundamental balance equations are given in Section 5, and the spheroid evolution is described in Section 6. The mathematical problem of existence of the solution after the onset of the liquid core is studied in Section 7. Section 8 describes the steady state, and some numerical simulations of the spheroid growth are illustrated in Section 9.

2 Model assumptions

The main assumptions made in [20], and still maintained in the present paper, are listed below:

- Throughout the spheroid just two components occupy volume: cells (independently of their state) and interstitial liquid. From the mechanical point of view the spheroid is considered to be a mixture of two incompressible fluids: the extracellular fluid, schematized as an inviscid fluid, and a different kind of fluid (to be specified) representing the cells. Their mutual interaction is assumed to be consistent with the possibility of describing the liquid/cell relative motion by means of Darcy's law.

- The spheroid is partitioned in a viable region and in a necrotic core. The interface is identified as the surface where the limiting nutrient (oxygen) takes a given critical value.
- The viable region is divided in an outer proliferating shell and an inner quiescent region, the interface being the surface where oxygen concentration crosses a given threshold for proliferation.
- The necrotic core is also partitioned in a "liquid" core (namely an immobile region at uniform pressure), surrounded by an outer shell whose mechanical behaviour is still described according to a two-fluid scheme. This picture is the consequence of an extreme idealization of the dead cells degrading process, turning "solid" cells to "liquid" (i.e. destroying their membrane and intracellular organelles) in a given finite time θ_D.
- Throughout the viable region and the "solid" necrotic zone the cells adhere to each other, and the volume fraction they occupy, ν, is constant.
- Both the cell velocity field $\mathbf{u}$ and the extracellular liquid velocity field $\mathbf{v}$ are radially directed and depend on the radial coordinate r only (of course also on time t if we consider evolution).
- A surface tension effect is postulated at the outer spheroid surface.
- The spheroid metabolism enters the model just through oxygen consumption.

While an external proliferating zone always exists, the presence of the other regions depends on the spheroid size. In fact, during the spheroid evolution from an early fully proliferating stage, the various interfaces will be generated progressively.

The partition of the necrotic zone into a "liquid" core and a "solid" shell may look arbitrary. Nevertheless, there is some experimental evidence that our picture may be realistic. Nuclear magnetic resonance (NMR) measurements of self-diffusion of water in EMT-6 spheroids [38] have shown that the central necrotic core looks as a single compartment characterised by a single diffusion coefficient, whereas the water in the viable rim appears to be confined into two compartments with different diffusion coefficients (intracellular and extracellular water). Moreover, NMR imaging evidences an intermediate zone between the viable rim and the centre of the necrotic region. This intermediate zone also shows two diffusion compartments, although the volume fraction of the diffusion-restricted compartment was found to be lower than the corresponding fraction in the viable rim.

Both in [23] and in most of [20], in the framework of the two-fluid model, all shear stresses are attributed to the viscosity of the cellular fluid. Actually, cells mutually interact not just by friction, but through links that are broken and reconstituted to allow some relative motion while keeping cells in mutual contact. The time scale of the regeneration of intercellular links is much shorter than the one of the flow. This is a strong motivation to propose an alternative description of the cell aggregate as a *Bingham fluid* (characterized by the presence of an yield stress) rather than a Newtonian fluid, an idea that was already discussed to some extent in [2, 41] and marginally brought forward in [20]. As we shall see in the next Section, adapting the Bingham scheme to the growing spheroid is a rather delicate question. Concerning the mechanical behaviour of the necrotic region, we note that cell death will eventually switch off the mechanism of replacement of the adhesion molecules on the cell membrane. We suppose that this phenomenon is faster than the membrane disruption, responsible for the later disappearance of viscosity. Summarizing, in our model we assume that:

- In the viable region the cell fluid is represented as a Bingham fluid with a constant yield stress. In the solid necrotic region the yield stress decreases linearly with the cell age counted from cell death, reaching zero at the age $\theta_\tau \leq \theta_D$.

If $\theta_\tau < \theta_D$, in the part of solid necrotic region where the yield stress is absent, the cell fluid is considered to be Newtonian .

Clearly, all disaggregation processes are progressive and randomly distributed in time and we are just arguing in terms of comparisons between the time scales of different phenomena. The problem arises of how to define viscosity in the necrotic region. It is certainly variable and decreasing inwards, but it would be anyway arbitrary to speculate about such a detail. In our view, the "solid" necrotic region is the one in which we can still count cells in an aggregate. Once aggregation is lost, most probably because of the membrane degradation, the system comes to rest and stress is isotropic.

Unlike most of the papers using the two-fluid scheme, here we have assumed the additional simplification of the constancy of the local cell volume fraction ν. Indeed in the two-fluid models it is customary to postulate a one-to-one correspondence between ν and the so-called *extra-pressure* acting on cells as a consequence of their mutual contact, in addition to the one exerted by the liquid. Such an approach implies the necessity of defining a potential for cell-cell interaction. Instead, we require

- The pressure p_C of the cell fluid is larger than the pressure p_E of the extracellular liquid.

This requirement, as we shall see, implies a constraint on the parameters. It is motivated by the fact that tractions cannot be properly accounted for in a two-fluid scheme (see also [33]).

We have adopted the assumption $\nu =$ constant not just because of its simplicity, but also because models involving a finer description of cell-cell interactions require the knowledge of hardly measurable parameters. The advantage of imposing the constraint $\nu =$ constant is quite substantial, since in that case, before the onset of the liquid necrotic core, both the kinetic fields $\mathbf{u}$ and $\mathbf{v}$ can be calculated explicitly in terms of the location of the various interfaces (in turn to be found by solving the oxygen diffusion-consumption problem). The inspiring principle is that simplicity is preferable to a more accurate picture that involves additional parameters whose determination is very uncertain. We recall that in [2], where Bingham-like schemes were considered in the more general framework of the theory of evolving natural configurations [31, 43], also elastic properties have been superimposed, according to the assumed variability of the cell volume fraction. Such a deformability is not allowed in our case.

It is important to note that, under the constraint ν = constant, growth is the only cause of shear rate. It is also important to point out that, in the context of a constant cell volume fraction, we are forced to introduce an analysis of stresses only because of the appearance of an inner liquid necrotic core. Models in which the whole necrotic core is assumed to keep a constant cell volume fraction while cells degrade to liquid, i.e. it is “solid”, need no stress computation since the cell velocity field can be derived just from the mass balance [28, 1, 15, 19, 8, 7]. The drawback of such an approach is that it implicitly requires the existence of some mechanism that forces mutual cell contact during the whole degradation process, which is hard to justify on a biophysical basis.

A substantial criticism might be addressed to selecting oxygen concentration as the discriminating quantity for the onset of necrosis. As a matter of fact cell metabolism is far more complicated to be reducible to just oxygen consumption. For instance, both insufficient ATP production rate and high acidity level (related to the anaerobic pathway of glucose consumption) can be considered responsible for necrosis occurrence. Such aspects have indeed received a lot of attention in the recent literature [47, 10, 11, 45, 44, 12]. We decided to keep the naive picture of one limiting nutrient to avoid accumulation of phenomena that are intrinsically difficult to model. Such a choice allows instead to emphasize the mechanical aspects. A similar argument can be brought to justify the introduction of an interface between the proliferating and the quiescent region, instead of some transition law between the two species, regulated by oxygen concentration.

Finally we note that the presence of intercellular bonds allows the onset of tensile stresses. To such action it is usually attributed a surface tension effect at the outer surface of the spheroid, which is known to play an important role in the two-fluid scheme. While adopting a two-fluid scheme we are still borrowing, perhaps with excessive ease, some concepts from solid mechanics: for instance, the implicit use of tensile stresses in the definition of surface tension, and the use of Darcy’s law to describe the motion of the extracellular liquid relative to the cells. This choice not only characterizes the cells as the solid matrix in a porous medium, but it also attributes a viscosity to the extracellular fluid, otherwise treated as inviscid (it is true, however, that its viscosity is many order of magnitude less than the one of the cell fluid).

3 The Bingham model

In the spirit of mixture theory (see [42]) the Cauchy stress tensor $\mathbf{T}$ in the spheroid is the sum of two tensors $\mathbf{T}_E$, $\mathbf{T}_C$, associated to the extracellular fluid and to the cell aggregate, respectively. We recall that the cell volume fraction ν is taken constant and that the density of the liquid and of the cells is considered equal. As we said, extracellular fluid is modelled as an inviscid fluid. Therefore, the corresponding stress tensor is simply

$$\mathbf{T}_E = (1-\nu)\big[-p_E\mathbf{I}\big]\,, \tag{1}$$

where p_E is the pressure and $\mathbf{I}$ is the identity tensor.

Passing to modelling the cellular fluid, we make a preliminary remark. Let $\mathbf{u}$ be the cell velocity field. We denote by $\mathbf{D} = \frac{1}{2}[\nabla\mathbf{u} + (\nabla\mathbf{u})^T]$ the strain rate tensor and by $I\!I_D$ the frame invariant quantity

$$I\!I_D = \frac{1}{2}\mathrm{Tr}\mathbf{D}^2\,. \tag{2}$$

If we take a constitutive law of the type

$$\mathbf{T}_C = \nu\big[-p_C\mathbf{I} + \lambda(I\!I_D)(\mathrm{Tr}\mathbf{D})\mathbf{I} + 2\eta_C(1+\vartheta(I\!I_D))\mathbf{D})\big]\,,$$

when the above defined invariant of the stress tensor exceeds some threshold, we are faced in particular with the problem of selecting the coefficient $\lambda(I\!I_D)$ (leaving aside for the moment the definitions of the positive coefficient η_C and of the function $\vartheta(I\!I_D)$. It is well known that this problem is linked to the entangled question of defining a bulk viscosity. We consider the decomposition $\mathbf{D} = \mathbf{D}' + \frac{1}{3}(\mathrm{Tr}\mathbf{D})\mathbf{I}$ and we impose that any non-rigid motion must be accompanied by energy dissipation, meaning that $\tilde{\mathbf{T}}_C{:}\mathbf{D} > 0$, where $\tilde{\mathbf{T}}_C = \mathbf{T}_C + \nu p_C\mathbf{I}$. Since

$$\frac{1}{\nu}\tilde{\mathbf{T}}_C{:}\mathbf{D} = 2\eta_C(1+\vartheta(I\!I_D))\mathbf{D}'{:}\mathbf{D}' + \big[\lambda(I\!I_D) + \frac{2}{3}\eta_C(1+\vartheta(I\!I_D))\big](\mathrm{Tr}\mathbf{D})^2\,,$$

it turns out that the factor multiplying $(\mathrm{Tr}\mathbf{D})^2$ must be non-negative. When $\vartheta = 0$ (Newtonian fluids) the customary choice is $\lambda + \frac{2}{3}\eta_C = 0$ (Stokes' assumption), which amounts to supposing that variations of specific volume are not dissipative, thus minimizing dissipation.

The presence of a yield stress for Bingham fluids ($\vartheta > 0$) suggests that in the expression of the energy dissipation rate the term $\frac{2}{3}\eta_C\vartheta(I\!I_D)(\mathrm{Tr}\mathbf{D})^2$ should be kept, since the corresponding volume increment rate in the spheroid is anyway associated with bonds rupture, and is therefore accompanied by the loss of some energy (the one accumulated in the bonds tension before rupture). At the same time we keep the assumption $\lambda = -\frac{2}{3}\eta_C$, eliminating the viscosity contribution to dissipation caused by volume changes. In the ordinary case of incompressible fluids ($\mathrm{Tr}\mathbf{D} = 0$) the choice of the parameter λ is clearly immaterial. In the case of spheroids, while the overall system remains incompressible, mass conversion from extracellular fluid to cells during proliferation produces a nonvanishing $\mathrm{Tr}\mathbf{D}$, accompanied by energy dissipation.

The above remarks are the motivation of the following Bingham-like model that was proposed in [20]. The cellular Cauchy stress tensor in the viable region is given by

$$\mathbf{T_C} = -\nu \left(p_C + \frac{2}{3}\eta_C \nabla \cdot \mathbf{u} \right) \mathbf{I} + \nu\tau \,, \tag{3}$$

where

$$\tau = \left(2\eta_C + \frac{\tau_0}{\sqrt{II_D}} \right) \mathbf{D} \tag{4}$$

if $\sqrt{II_\tau} > \tau_0$, while $\mathbf{D} = 0$ otherwise. Note that, for $\mathbf{D} \neq 0$,

$$\sqrt{II_\tau} = 2\eta_C \sqrt{II_D} + \tau_0, \qquad \text{if } II_D > 0 \,. \tag{5}$$

More complicated variants have been considered in [2], which are suitable to the mechanical framework of that paper, using in place of $\mathbf{D}$ the strain rate tensor corresponding to deformations not simply attributable to growth and that therefore are by definition traceless. When $\nabla \cdot \mathbf{u} > 0$, as it happens in the presence of proliferation, the question of formulating a Bingham-like model in a self-consistent way is far from being obvious. For instance, in [4] the authors propose that for Bingham flows which are not divergence free a possible choice can be (using our symbols)

$$\tilde{\mathbf{T}} = \nu \left(1 + \frac{\tau_0}{\varphi(-\frac{2}{3}\eta_C \mathrm{Tr}\mathbf{D}\,\mathbf{I} + 2\eta_C \mathbf{D})} \right) \left(-\frac{2}{3}\eta_C \mathrm{Tr}\mathbf{D}\,\mathbf{I} + 2\eta_C \mathbf{D} \right) \,,$$

where φ is simply the square root of the invariant of its argument, according to (2). However, it is easy to check that for a radial velocity field of the form $\mathbf{u} = k\mathbf{r}$ the function φ vanishes, while the tensor $\mathbf{D}$ does not, and this is certainly not suitable for our modelling (by the way, that kind of velocity field is precisely the one arising in the first stage of evolution, in which the whole spheroid is proliferating). The constitutive law we have selected bypasses that difficulty, since II_D in the form (2) vanishes if and only if $\mathbf{D} = 0$.

Finally, we remark that in Eqs. (1) and (3) different pressures were considered for the two phases. This is consistent with the fact that, either because of surface tension or by external actions applied selectively to the cells, the two pressures can take different values at the outer surface. This is clearly another contradiction to the two-fluid scheme which we add to our list of compromises.

4 Oxygen consumption and the inner structure of the spheroid

The oxygen diffusion-consumption problem can be considered quasi-steady with excellent approximation, due to the large diffusivity of oxygen ($1.82 \cdot 10^{-5}\,\mathrm{cm}^2/\mathrm{s}$ [35]) in the system and the relative small size of the tumour spheroid (external radius not much larger than $1\,\mathrm{mm}$). Thus it can be solved at each time t if the spheroid radius $R(t)$ is known.

We partition the spheroid according to the value of the oxygen concentration σ. Denoting by σ^* the concentration at $r = R(t)$, in a generic configuration we distinguish the following regions:

- (P) proliferating region, $\rho_P(t) < r < R(t)$, corresponding to $\sigma_P < \sigma < \sigma^*$;
- (Q) quiescent region, $\rho_N(t) < r < \rho_P(t)$, corresponding to $\sigma_N < \sigma < \sigma_P$;
- (N) necrotic region, $0 < r < \rho_N(t)$, corresponding to $\sigma \leq \sigma_N$.

The interfaces ρ_P, ρ_N may or may not exist, depending on the size of the spheroid. Assuming $\sigma^* > \sigma_P$, the concentration σ and the various interfaces for R large enough are found by solving the following free boundary problem:

$$D_{O_2}\Delta\sigma(r,t) = f(\sigma(r,t))\nu, \qquad \text{in } P\,, \tag{6}$$

$$D_{O_2}\Delta\sigma(r,t) = \frac{1}{m}f(\sigma(r,t))\nu, \qquad \text{in } Q\,, \tag{7}$$

$$\sigma(R,t) = \sigma^*\,, \tag{8}$$

$$\sigma(\rho_P,t) = \sigma_P\,, \tag{9}$$

$$\sigma(\rho_N,t) = \sigma_N\,, \tag{10}$$

$$\sigma_r(\rho_N,t) = 0\,, \tag{11}$$

where $f(\sigma)$ is a Michaelis-Menten type function and $m > 1$ (quiescent cells need less oxygen than proliferating cells). The last condition expresses no oxygen flux to the necrotic core. The problem has a hidden additional unknown, which is the spheroid external moving boundary $r = R(t)$.

Remark 4.1 *We have already noticed that partitioning the spheroid according to oxygen concentration is a rather extreme picture, that contrasts with the stochastic nature of the various processes involved. In particular, transition rates from one class to another (not only between P and Q, but also from P, Q to N) are usually introduced [27]. The interfaces are generated by a limiting procedure, sharpening thin transition regions.*

In the papers [8, 9] we have discussed a similar free boundary problem for the pair $(\sigma, \rho_N(t))$ (with overlapping regions P, Q). The extension to the present case is not difficult. We can summarize the main results concerning problem (6)-(11) in the following statement.

Theorem 4.1 *There exist two monotonically increasing continuous functions $R_P(\sigma^*)$, $R_N(\sigma^*)$ such that:*

i. for $R(t) \leq R_P$ system (6),(8), with the additional condition $\sigma_r(0,t) = 0$, has one unique solution $\sigma(r,t) > \sigma_P$;

ii. for $R_P < R(t) \leq R_N$ there exists one unique pair $\sigma(r,t), \rho_P(t)$ solving (6)-(9) with $\sigma_r(0,t) = 0$, i.e. the necrotic region has not yet appeared;

iii. for $R(t) > R_N$ there exists one unique triple, $\sigma(r,t), \rho_P(t), \rho_N(t)$, solving (6)-(11). ☐

It is clear that ρ_P and ρ_N are functions of the radius R, and that they actually depend on t through $R(t)$.

We will write the right hand side of (6) in the form

$$f(\sigma, \nu) = nQ\frac{\sigma}{H+\sigma}\,,$$

where Q is the maximum oxygen consumption rate per cell and n is the cell concentration. In the following simulation we will take $Q = 8.3 \cdot 10^{-17}\,\mathrm{mol/(cell{\cdot}s)}$ [25], $n = 5 \cdot 10^8$ cell/cm^3 [25], $H = 4.64 \cdot 10^{-3}\,\mathrm{mM}$ [18], $m = 2$ [13], $D = 1.82 \cdot 10^{-5}\mathrm{cm}^2/\mathrm{s}$ [35], $\sigma_P = 0.05\,\mathrm{mM}$, $\sigma_N = 0.01\,\mathrm{mM}$. Fig. 1 shows the radii ρ_P, ρ_N as functions of R, in case of $\sigma^* = 0.28\,\mathrm{mM}$ [26]. Note that the differences $R - \rho_P$ and $\rho_N - \rho_N$ tend to be constant for R large enough.

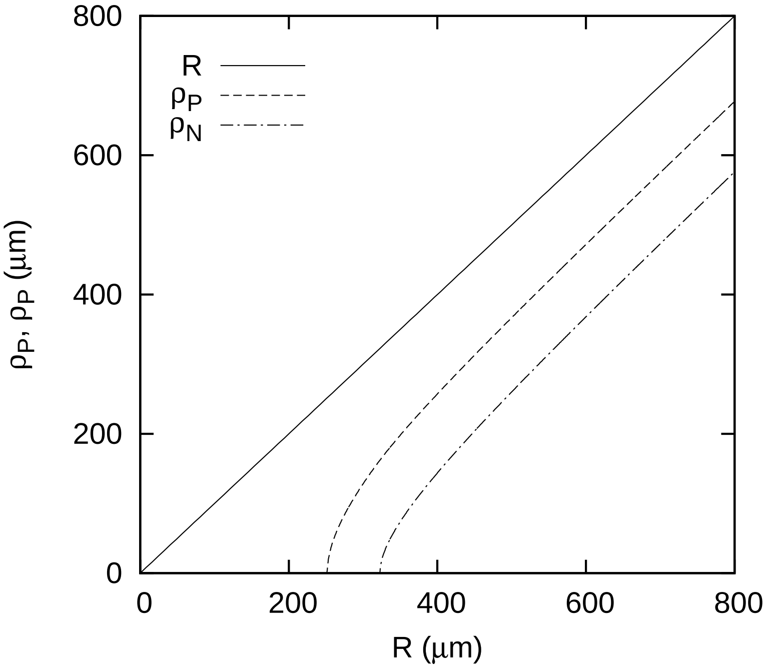

Figure 1: ρ_P and ρ_N as a functions of R. Parameter values indicated in the text.

We still have to deal briefly with the necrotic region. In a generic configuration, we suppose that it contains a "liquid" core (region NL) for $0 < r < \rho_D(t)$, meaning just a region of uniform pressure, and a "solid" shell (region NS) for $\rho_D(t) < r < \rho_N(t)$, having the mechanical properties of a mixture of cells in mutual contact and extracellular liquid. Such a picture comes from the idea that, (a) as long as dead cells have a membrane, we can still use a mechanical scheme similar to that adopted for living cells, while membrane degradation leads to a uniform incompressible material, and (b) from the assumption that all necrotic cells undergo degradation after the same time θ_D.

To the region NS we extend most of the properties of the viable zone, in particular the constancy of the cell volume fraction ν (with the same value). We do not take for NS exactly the same rheological properties we attributed to the viable region, since intercellular bonds are also degrading. As stated above, we take in NS a Bingham model with a yield stress gradually going to zero.

According to the picture above, the interface $r = \rho_D(t)$ is located by following the motion of cells as they enter the necrotic region and computing how long they travel during the prescribed degradation time θ_D. Such a calculation requires the knowledge of the velocity field, and will be done later on. Of course the liquid core will appear only when the spheroid has grown sufficiently large.

5 Balance equations

From the mass balance, and assuming the same mass density for the cells and the liquid, we obtain the following equations:

$$\nabla \cdot \mathbf{u} = \chi, \qquad \text{in } P, \tag{12}$$

$$\nabla \cdot \mathbf{u} = 0, \qquad \text{in } Q \cup NS, \tag{13}$$

$$\nabla \cdot \mathbf{v} = -\chi \frac{\nu}{1-\nu}, \qquad \text{in } P, \tag{14}$$

$$\nabla \cdot \mathbf{v} = 0, \qquad \text{in } Q \cup NS \cup NL. \tag{15}$$

The above equations express the incompressibility of the mixture, since we have

$$\nabla \cdot [\nu \mathbf{u} + (1-\nu)\mathbf{v}] = 0\,,$$

which provides a simple relationship between $\mathbf{u}$ and $\mathbf{v}$. It turns out that the total flux $\nu\mathbf{u} + (1-\nu)\mathbf{v}$ is identically zero during the whole process, so that

$$\mathbf{v} = -\frac{\nu}{1-\nu}\mathbf{u}\,. \tag{16}$$

Concerning the momentum balance, since inertia is absolutely negligible and $\mathbf{T}_C$ and $\mathbf{T}_E$ are given by Eqs. (3) and (1), respectively, in all regions which are not static we write the equations

$$\nabla \cdot \mathbf{T}_C + \mathbf{m}_C = \mathbf{0}\,, \tag{17}$$

$$\nabla \cdot \mathbf{T}_E + \mathbf{m}_E = \mathbf{0}\,, \tag{18}$$

where $\mathbf{m}_C$, $\mathbf{m}_E$ are the interaction forces between the components. By assuming that the motion of the liquid relative to the cells is governed by Darcy's law we have

$$\mathbf{v} - \mathbf{u} = -K\nabla p_E\,, \tag{19}$$

with $(1-\nu)K$ representing the hydraulic conductivity. Arguing as in [20], we conclude that

$$\mathbf{m}_E = \frac{\mathbf{u}}{K} \tag{20}$$

and, with very good approximation,

$$\mathbf{m}_C + \mathbf{m}_E = 0\,, \tag{21}$$

since the interaction force generated by the momentum exchange rate between the species is negligible.

In the following we have to write down equations (17), (18). To this end we must keep in mind that in our polar coordinate frame of reference and for any radial velocity field $u(r,t)$:

- the tensor $\mathbf{D}$ is diagonal: $\mathbf{D} = \mathrm{Diag}(\frac{\partial u}{\partial r}, \frac{u}{r}, \frac{u}{r})$;
- $\mathrm{Tr}\mathbf{D} = \nabla \cdot \mathbf{u}$ is either χ or 0, depending on whether proliferation is active or not;
- $II_D = \frac{1}{2}\big(\frac{\partial u}{\partial r}\big)^2 + \big(\frac{u}{r}\big)^2$;
- $(\nabla \cdot \mathbf{D})_r = \Delta u - 2\frac{u}{r^2}$, $\quad (\nabla \cdot \mathbf{D})_\theta = (\nabla \cdot \mathbf{D})_\phi = 0$;
- $\nabla \cdot \mathbf{u} \equiv$ constant implies $\nabla \cdot \mathbf{D} = 0$;
- where $\nabla \cdot \mathbf{D} = 0$, we have

  $$\left(\nabla \cdot \left[(2\eta_C + \frac{\tau_0}{\sqrt{II_D}})\mathbf{D}\right]\right)_r = \frac{\tau_0}{\sqrt{II_D}}\left(-\frac{1}{2II_D}\frac{\partial II_D}{\partial r}\right)\frac{\partial u}{\partial r}\,, \tag{22}$$

  and the other components are zero.

The presence of motion indicates that stress is beyond the threshold, so that (3) has to be applied.

We establish now the expression of the cellular pressure at $r = R$. If the spheroid is grown in water, then the external normal stress reduces to the atmospheric pressure p_{ext}. If the outer medium is a gel [30], then an extra compression due to the deformation of the polymer network forming the gel skeleton is exerted on the cells, i.e., on the solid component of the spheroid. Surface tension acts exclusively on the cells as well. While we just have pressure continuity for the liquid component, the boundary condition for p_C can be stated by imposing a jump condition, accounting for the surface tension, to the total stress in the radial direction. So, using $(\cdot)' = \frac{\partial \cdot}{\partial r}$, we can write

$$-\nu\left(p_C(R,t) + \frac{2}{3}\eta_C\chi\right) + \nu\left(2\eta_C + \frac{\tau_0}{\sqrt{II_D(R,t)}}\right)u'(R,t) - (1-\nu)p_{ext} =$$
$$-p_{ext} - \nu\psi(R) - \nu\frac{2\gamma}{R}\,,$$

where γ is the surface tension and $\psi(R)$ is a function that represents the gel action, increasing from 0 for $R = 0$ to some upper value ψ_{max} (the gel has a plastic behaviour, since its internal polymeric network breaks when deformed beyond some limit). From the above equation we have

$$p_C(R,t) = -\frac{2}{3}\eta_C\chi + \left(2\eta_C + \frac{\tau_0}{\sqrt{II_D(R,t)}}\right) u'(R,t) + p_{ext} + \psi(R) + \frac{2\gamma}{R}\,. \tag{23}$$

Remark 5.1 *Surface tension related pressure can be given the form $2\gamma/R$ (with γ constant) only if R is sufficiently large. When R becomes very small the tensile stresses producing such a pressure are no longer present. So if we want to keep that term, γ should be considered a function of R which vanishes for $R \to 0$, e.g. quadratically, and is constant for R sufficiently large.*

6 Spheroid evolution

6.1 Stage I

In the first stage of evolution only the P zone is present and Eq. (12) holds with zero velocity at the centre. Thus

$$u(r,t) = \frac{\chi}{3}r\,. \tag{24}$$

As a consequence, the outer boundary, which is a material surface, moves according to

$$\dot{R}(t) = \frac{\chi}{3}R(t)\,. \tag{25}$$

If R_0 is the initial radius, we have the exponential growth

$$R(t) = R_0 \exp\left(\frac{\chi}{3}t\right), \tag{26}$$

and Stage I will end at the time

$$t_P = \frac{3}{\chi}\ln\left(\frac{R_P}{R_0}\right),$$

when quiescence first appears at the centre.

For the velocity field (24) we have

$$\mathbf{D} = \frac{\chi}{3}\mathbf{I}\,, \qquad II_D = \frac{\chi^2}{6}\,,$$

$$\nabla\cdot\tau = \nabla\cdot\mathbf{D} = \mathbf{0}\,.$$

The tensor $\mathbf{T}_C$ is

$$\mathbf{T_C} = -\nu\left(p_C + \frac{2}{3}\eta_C\chi\right)\mathbf{I} + \nu\left(2\eta_C + \frac{\sqrt{6}\tau_0}{\chi}\right)\mathbf{D}\,, \tag{27}$$

and equation (17) becomes (nonradial components are trivial)

$$\nu \nabla p_C + \frac{\chi}{3K} r = 0 \,. \tag{28}$$

From (28) we obtain

$$p_C(r,t) = p_C(R,t) + \frac{\chi}{6K\nu}(R^2 - r^2)\,, \tag{29}$$

and, recalling (23),

$$p_C(r,t) = \tau_0 \sqrt{\frac{2}{3}} + p_{ext} + \psi(R) + \frac{2\gamma}{R} + \frac{\chi}{6K\nu}(R^2 - r^2)\,. \tag{30}$$

Similarly, from (18) we get

$$p_E(r,t) = p_{ext} - \frac{\chi}{6K(1-\nu)}(R^2 - r^2)\,. \tag{31}$$

6.2 Stage II

For $t > t_P$, a quiescent core with $0 < r < \rho_P(t)$ grows, where cells have no velocity in view of (13) and of $u(0,t) = 0$. In the region P equation (12) has to be integrated, imposing that u vanishes at $r = \rho_P(t)$. Thus

$$u(r,t) = \frac{\chi}{3} r \big[1 - (\frac{\rho_P(t)}{r})^3\big]\,. \tag{32}$$

From the previous section we recall that $\rho_P(t)$ can be found as a continuous, though not explicit, function of $R(t)$. Therefore, the equation for the motion of the outer boundary

$$\dot{R}(t) = \frac{\chi}{3} R(t) \big[1 - (\frac{\rho_P(t)}{R(t)})^3\big] \tag{33}$$

can be integrated (numerically), knowing that $R = R_P$ at time $t = t_P$. Stage II comes to an end at the time $t = t_N$ when R reaches the value R_N and necrosis first appears at $r = 0$.

For the velocity field (32) in the region P we have

$$II_D = \frac{\chi^2}{3}\big[\frac{1}{2} + (\frac{\rho_P}{r})^6\big]\,. \tag{34}$$

Equation (17), in view of (22), becomes

$$-p_C' + \tau_0 u' (\frac{1}{\sqrt{II_D}})' - \frac{u}{\nu K} = 0\,. \tag{35}$$

To integrate the above equation from r to R, we perform the integration by parts:

$$\int_r^R u' (\frac{1}{\sqrt{II_D}})' \, ds = u' \frac{1}{\sqrt{II_D}} \Big|_r^R - \int_r^R \frac{u''}{\sqrt{II_D}} \, ds\,,$$

with

$$\int_r^R \frac{u''}{\sqrt{II_D}}\,ds = -2\sqrt{3}\int_r^R \frac{\frac{1}{s}\big(\frac{\rho_P}{s}\big)^3}{\big[\frac{1}{2}+\big(\frac{\rho_P}{s}\big)^6\big]^{1/2}}\,ds\,.$$

For $\rho_P(t) < r < R(t)$, integrating (35) we can write

$$\begin{aligned} p_C(r,t) =& p_C(R,t) - \frac{\tau_0}{\sqrt{3}}\Big\{\sqrt{2}\frac{1+2\big(\frac{\rho_P}{s}\big)^3}{\big[1+2\big(\frac{\rho_P}{s}\big)^6\big]^{1/2}}\Bigg|_r^R - 2\ln\Big[\big(\frac{\rho_P}{s}\big)^3 + \big[\frac{1}{2}+\big(\frac{\rho_P}{s}\big)^6\big]^{1/2}\Big]\Bigg|_r^R\Big\} \\ &+\frac{\chi}{3\nu K}\Big[\frac{R^2-r^2}{2}+\rho_P^3\big(\frac{1}{R}-\frac{1}{r}\big)\Big]\,, \end{aligned} \tag{36}$$

where

$$p_C(R,t) = \frac{4}{3}\eta_C\chi\left(\frac{\rho_P}{R}\right)^3 + \tau_0\sqrt{\frac{2}{3}}\frac{1+2\left(\frac{\rho_P}{R}\right)^3}{\left[1+2\left(\frac{\rho_P}{R}\right)^6\right]^{1/2}} + p_{ext} + \psi(R) + \frac{2\gamma}{R}\,. \tag{37}$$

For $0 < r < \rho_P(t)$, i.e. in the region Q, we have $u(r,t) = 0$ and then $\mathbf{D} = 0$. Therefore $\mathbf{T}_C = -\nu p_C \mathbf{I}$, from which we deduce $\nabla p_C = 0$ and then $p_C(r,t) \equiv p_C(\rho_P^-,t)$. To derive the value of $p_C(\rho_P^-,t)$, we impose the continuity of the normal stress at $r = \rho_P$. Taking into account the continuity of the extracellular liquid pressure, we prescribe

$$-\Big[p_C(\rho_P^+,t)+\frac{2}{3}\eta_C\chi\Big] + \left(2\eta_C + \frac{\tau_0}{\sqrt{II_D}}\right)\Bigg|_{r=\rho_P^+} u'(\rho_P^+,t) = -p_C(\rho_P^-,t)\,. \tag{38}$$

From the above equation we obtain the extent of the pressure jump at $r = \rho_P$

$$p_C(\rho_P^+,t) - p_C(\rho_P^-,t) = \frac{4}{3}\eta_C\chi + \sqrt{2}\tau_0\,. \tag{39}$$

Thus, we get the complete profile of $p_C(r,t)$:

$$\begin{aligned} p_C(r,t) =& \frac{4}{3}\eta_C\chi\left(\frac{\rho_P}{R}\right)^3 + p_{ext} + \psi(R) + \frac{2\gamma}{R} \\ &+\frac{\chi}{3\nu K}(R-r)\Big(\frac{R+r}{2}-\frac{\rho_P^3}{rR}\Big) \\ &+\tau_0\sqrt{\frac{2}{3}}\Big\{\frac{1+2\big(\frac{\rho_P}{r}\big)^3}{\big[1+2\big(\frac{\rho_P}{r}\big)^6\big]^{1/2}} + \sqrt{2}\ln\Big[\big(\frac{\rho_P}{s}\big)^3 + \big[\frac{1}{2}+\big(\frac{\rho_P}{s}\big)^6\big]^{1/2}\Big]\Bigg|_r^R\Big\}\,, \end{aligned} \tag{40}$$

for $\rho_P < r \le R$, and

$$p_C(r,t) = p_C(\rho_P^+,t) - \frac{4}{3}\eta_C\chi - \sqrt{2}\tau_0\,, \tag{41}$$

for $0 \le r < \rho_P$. Concerning the extracellular fluid pressure, we have

$$p_E(r,t) = \begin{cases} p_{ext} - \dfrac{\chi}{3K(1-\nu)}(R-r)\Big(\dfrac{R+r}{2}-\dfrac{\rho_P^3}{rR}\Big), & \rho_P \le r \le R; \\ \\ p_E(\rho_P,t), & 0 < r < \rho_P. \end{cases} \tag{42}$$

In conclusion, moving inwards from the periphery, the cell pressure p_C increases in region P, drops crossing ρ_P and remains constant in Q. The liquid pressure p_E, instead, decreases in P and is constant in Q.

Finally, we may compare the two pressure fields. For $\rho_P < r \leq R$ we have

$$\begin{aligned} p_C(r,t) - p_E(r,t) =& \frac{4}{3}\eta_C\chi\left(\frac{\rho_P}{R}\right)^3 + \psi(R) + \frac{2\gamma}{R} \\ &+ \frac{\chi}{3\nu(1-\nu)K}(R-r)\Big(\frac{R+r}{2} - \frac{\rho_P^3}{rR}\Big) \\ &+ \tau_0\sqrt{\frac{2}{3}}\Big\{\frac{1+2\big(\frac{\rho_P}{r}\big)^3}{\sqrt{1+2\big(\frac{\rho_P}{r}\big)^6}} + \sqrt{2}\ln\frac{\big(\frac{\rho_P}{R}\big)^3 + \sqrt{\frac{1}{2}+\big(\frac{\rho_P}{R}\big)^6}}{\big(\frac{\rho_P}{r}\big)^3 + \sqrt{\frac{1}{2}+\big(\frac{\rho_P}{r}\big)^6}}\Big\}, \end{aligned} \tag{43}$$

and, for $0 \leq r < \rho_P$,

$$\begin{aligned} p_C(r,t) - p_E(r,t) =& \frac{2\gamma}{R} + \psi(R) - \frac{4}{3}\eta_C\chi\Big[1 - \Big(\frac{\rho_P}{R}\Big)^3\Big] \\ &+ \frac{\chi}{3\nu(1-\nu)K}(R-\rho_P)^2\Big(\frac{1}{2} + \frac{\rho_P}{R}\Big) \\ &- \frac{2}{\sqrt{3}}\tau_0\ln\frac{1+\sqrt{\frac{3}{2}}}{\Big(\frac{\rho_P}{R}\Big)^3 + \sqrt{\frac{1}{2}+\Big(\frac{\rho_P}{R}\Big)^6}}\,. \end{aligned} \tag{44}$$

We remark that if the condition $p_C > p_E$ is satisfied for $0 \leq r < \rho_P$, then it is satisfied also for $\rho_P < r \leq R$.

6.3 Stage III

As the spheroid radius increases, the oxygen concentration will reach the threshold σ_N at the time t_N. In the time interval $(t_N, t_N + \theta_D)$ the necrotic region consists of the subset NS only. Neither dead nor quiescent cells move, so that the boundary $r = \rho_P(t)$ carries the zero velocity condition, while (12) has to be integrated in the region P, yielding once more (32). The radius $R(t)$ still obeys (33). The pressures p_C and p_E take the same expressions (40), (41) and (42), as well as the difference $p_C - p_E$ is still given by (43), (44). Stage III ends at the time $t_D = t_N + \theta_D$, at which $R(t_D) = R_D$, when the region NL appears. The positivity of the r.h.s. of (44) for $R_P \leq R \leq R_D$ imposes a constraint on the parameters.

6.4 Stage IV

For $t > t_D$ the region NL will be present for r in the interval $(0, \rho_D)$, changing the whole structure of the velocity field, since we only know that the material filling the region NL has zero velocity, but we lose the boundary condition for u at $r = \rho_D$. The missing condition has to come from the stress analysis.

Let us introduce the unknown cell velocity at $r = \rho_N$ as a function of time, $\omega_N(t) = u(\rho_N(t), t)$, which is zero for $t_N \leq t < t_D$. By continuity, we put $\omega_N(t_D) = 0$. We are able to describe the whole kinematics in terms of ω_N, still remembering that ρ_N, ρ_P are functions of R via Eqs. (6)-(11):

$$u(r,t) = \frac{1}{r^2}\rho_N^2(t)\omega_N(t)\,, \qquad \rho_D \leq r \leq \rho_P\,, \tag{45}$$

$$u(r,t) = \frac{1}{r^2}\rho_N^2(t)\omega_N(t) + \frac{\chi}{3}\Big(r - \frac{\rho_P^3(t)}{r^2}\Big)\,, \qquad \rho_P \leq r \leq R\,. \tag{46}$$

From the above equations we obtain the differential equation for R:

$$R^2(t)\dot{R}(t) = \rho_N^2(t)\omega_N(t) + \frac{\chi}{3}(R^3(t) - \rho_P^3(t))\,. \tag{47}$$

In order to find ρ_D we integrate $r^2 u = \rho_N^2 \omega_N$, interpreting u as $\dot{r}$ with the condition $r|_{t-\theta_D} = \rho_N(t - \theta_D)$, obtaining

$$\frac{1}{3}[\rho_D^3(t) - \rho_N^3(t-\theta_D)] = \int_{t-\theta_D}^{t} \rho_N^2(\tau)\omega_N(\tau)\,d\tau\,. \tag{48}$$

Note that if $\omega_N = 0$ in $[t - \theta_D, t]$, then ρ_D is just a translation of ρ_N as expected.

Since we have assumed a linearly decreasing yield stress in the region NS, we have for the yield stress at the generic (r,t) the expression

$$\tilde{\tau}_0(r,t) = \begin{cases} \tau_0, & \rho_N \leq r \leq R; \\ \tau_0\big[1 - \frac{\theta(r,t)}{\theta_\tau}\big]_+, & \rho_D < r < \rho_N, \end{cases} \tag{49}$$

where $\theta(r,t)$ is the age from death of cells at position r and time t. The age $\theta(r,t)$ is defined implicitly by

$$\frac{1}{3}\big[r^3 - \rho_N^3(t - \theta(r,t))\big] = \int_{t-\theta(r,t)}^{t} \rho_N^2(\tau)\omega_N(\tau)\,d\tau\,. \tag{50}$$

If $0 < \theta_\tau < \theta_D$ a new boundary, $r = \rho_\tau(t)$, arises in NS between Bingham and Newtonian fluids and it is defined by

$$\frac{1}{3}\big[\rho_\tau^3(t) - \rho_N^3(t-\theta_\tau)\big] = \int_{t-\theta_\tau}^{t} \rho_N^2(\tau)\omega_N(\tau)\,d\tau\,. \tag{51}$$

This boundary obviously coincides with $r = \rho_D$ if $\theta_\tau = \theta_D$.

The condition allowing to determine ω_N for $t > t_D$ is the continuity of normal stress at $r = \rho_D$. In the inner liquid core the stress is uniform and isotropic and, since p_E is continuous across the interface, it reduces to the pressure $p_E(\rho_D, t)$. Therefore, the normal stress continuity at $r = \rho_D$ takes the form

$$\nu p_C(\rho_D^+, t) - 2\nu\eta_C u'(\rho_D^+, t) + (1-\nu)p_E(\rho_D, t) = p_E(\rho_D, t)\,,$$

that is,

$$p_C(\rho_D^+,t) - 2\eta_C u'(\rho_D^+,t) = p_E(\rho_D,t)\,. \tag{52}$$

We remark that, under the continuity of normal stress, we have $p_C(\rho_D^+,t) > p_E(\rho_D^+,t)$ if and only if $\omega_N(t) < 0$, which is a very natural physical condition. Since we require $p_C > p_E$ in all the "solid" spheroid, ω_N must be negative for $t > t_D$. On the other hand, it can be seen that if the inequality $p_C > p_E$ is satisfied at $r = \rho_D^+$, then it is satisfied also for $\rho_D < r \leq R$. So we can conclude that $\omega_N < 0$ for $t > t_D$ is necessary and sufficient to have $p_C > p_E$ for $\rho_D < r \leq R$ during the stage IV.

By computing the pressures p_C and p_E at $r = \rho_D$, as reported in the Appendix, and taking into account that we are looking for negative ω_N, (52) takes the following explicit expression:

$$\begin{aligned}\frac{2\gamma}{R} &= -\psi(R) + 4\eta_C\rho_N^2\omega_N\Big(\frac{1}{R^3}-\frac{1}{\rho_D^3}\Big) + \frac{4}{3}\eta_C\chi\Big[1-\Big(\frac{\rho_P}{R}\Big)^3\Big] \\ &- \frac{1}{\nu(1-\nu)K}\Big\{\rho_N^2\omega_N\Big(\frac{1}{\rho_D}-\frac{1}{R}\Big) + \frac{\chi}{3}(R-\rho_P)^2\Big(\frac{1}{2}+\frac{\rho_P}{R}\Big)\Big\} \\ &+ \frac{2}{\sqrt{3}}\tau_0\Bigg\{\ln\frac{\Big(\frac{\rho_P}{\rho_\tau}\Big)^3\Bigg[1+\sqrt{\dfrac{\chi^2\rho_P^6}{6\big(\frac{\chi}{\sqrt{3}}\rho_P^3-\sqrt{3}\rho_N^2\omega_N\big)^2}+1}\Bigg]}{\Big(\frac{\rho_P}{R}\Big)^3+\sqrt{\dfrac{\chi^2\rho_P^6}{6\big(\frac{\chi}{\sqrt{3}}\rho_P^3-\sqrt{3}\rho_N^2\omega_N\big)^2}+\Big(\frac{\rho_P}{R}\Big)^6}} - \frac{3}{\theta_\tau}\int_{\rho_\tau}^{\rho_N}\frac{\theta(r,t)}{r}\,dr\Bigg\}\end{aligned} \tag{53}$$

The spheroid evolution will then be described by the system of equations (47), (48), (50), (51), and (53), coupled with (6)-(11).

The whole profile of the pressures p_C and p_E could be computed, given ω_N, according to the same procedure followed for stages II and III. Here we only note that the cell pressure has a jump at $r = \rho_P$, given by Eq. (A.2) in Appendix, whereas it is continuous at $r = \rho_N$ and also at $r = \rho_\tau$ when $\theta_\tau < \theta_D$.

It can be of interest to consider the case $\theta_\tau \to 0$. In this case $\rho_\tau \to \rho_N$. By using the mean value theorem, for the integral in (53) we have

$$\frac{1}{\theta_\tau}\int_{\rho_\tau}^{\rho_N}\frac{\theta(r,t)}{r}\,dr = \frac{\rho_N(t)-\rho_\tau(t)}{\theta_\tau}\,\frac{\theta(\hat{r},t)}{\hat{r}}\,,\quad \hat{r}\in[\rho_\tau(t),\rho_N(t)]\,. \tag{54}$$

The first fraction in the r.h.s. of the previous equation can be rewritten as

$$\frac{\rho_N(t)-\rho_\tau(t)}{\theta_\tau} = \frac{\rho_N(t)-\rho_N(t-\theta_\tau)}{\theta_\tau} + \frac{\rho_N(t-\theta_\tau)-\rho_\tau(t)}{\theta_\tau}\,. \tag{55}$$

When $\theta_\tau \to 0$ the first addend in the r.h.s. of (55) tends to $\dot{\rho}_N(t)$, which is finite, whereas the second addend, taking into account (51) and factoring the difference

$\rho_\tau^3(t) - \rho_N^3(t-\theta_\tau)$, can be seen to have a finite limit. Therefore the limit of (54) is zero since $\hat{r} \to \rho_N(t)$ and $\theta(\rho_N, t) = 0$. Thus (53) reduces to

$$\begin{aligned}\frac{2\gamma}{R} &= -\psi(R) + 4\eta_C \rho_N^2 \omega_N \Big(\frac{1}{R^3} - \frac{1}{\rho_D^3}\Big) + \frac{4}{3}\eta_C \chi \Big[1 - \Big(\frac{\rho_P}{R}\Big)^3\Big] \\ &- \frac{1}{\nu(1-\nu)K}\Big\{\rho_N^2 \omega_N \Big(\frac{1}{\rho_D} - \frac{1}{R}\Big) + \frac{\chi}{3}(R-\rho_P)^2\Big(\frac{1}{2} + \frac{\rho_P}{R}\Big)\Big\} \\ &+ \frac{2}{\sqrt{3}}\tau_0 \ln \frac{\Big(\frac{\rho_P}{\rho_N}\Big)^3 \left[1 + \sqrt{\frac{\chi^2 \rho_P^6}{6\big(\frac{\chi}{\sqrt{3}}\rho_P^3 - \sqrt{3}\rho_N^2 \omega_N\big)^2} + 1}\,\right]}{\Big(\frac{\rho_P}{R}\Big)^3 + \sqrt{\frac{\chi^2 \rho_P^6}{6\big(\frac{\chi}{\sqrt{3}}\rho_P^3 - \sqrt{3}\rho_N^2 \omega_N\big)^2} + \Big(\frac{\rho_P}{R}\Big)^6}}\,. \end{aligned} \tag{56}$$

We note that, while $\lim_{\theta_\tau \to 0}(p_C(\rho_N^+, t) - p_C(\rho_N^-, t)) = 0$, the cell pressure at $r = \rho_N$ is no longer continuous for $\theta_\tau = 0$, exhibiting the jump

$$p_C(\rho_N^+, t) - p_C(\rho_N^-, t) = \frac{2}{\sqrt{3}}\tau_0\,. \tag{57}$$

The continuity of normal stress is still expressed by (56) (see Appendix).

Concerning the unknown $\omega_N(t)$, Eq. (53) confirms that $\omega_N(t_D) = 0$. Indeed, in the opposite case the singularities ω_N/ρ_D^3 and ω_N/ρ_D appearing in (53) for $t \to t_D^+$ could not be balanced by any other term. We have in fact:

Proposition 6.1 *The ratio ω_N/ρ_D^3 is bounded as $t \to t_D^+$.*

Proof If $0 < \theta_\tau < \theta_D$, let us take the limit as $t \to t_D^+$ ($\rho_D \to 0^+$) in (53), and set $z_0 = \lim_{t \downarrow t_D} \frac{\omega_N}{\rho_D^3}$. Arguing as if z_0 is bounded, then $\lim_{t \downarrow t_D} \frac{\omega_N}{\rho_D} = 0$. So we obtain

$$\begin{aligned}\frac{2\gamma}{R} &= -\psi(R) - 4\eta_C \rho_N^2 z_0 + \frac{4}{3}\eta_C \chi \Big[1 - \Big(\frac{\rho_P}{R}\Big)^3\Big] \\ &- \frac{1}{\nu(1-\nu)K}\frac{\chi}{3}(R-\rho_P)^2\Big(\frac{1}{2} + \frac{\rho_P}{R}\Big) \\ &+ \frac{2}{\sqrt{3}}\tau_0 \left\{\ln\left[\Big(\frac{\rho_P}{\rho_\tau}\Big)^3 \frac{1 + \sqrt{\frac{3}{2}}}{\Big(\frac{\rho_P}{R}\Big)^3 + \sqrt{\frac{1}{2} + \Big(\frac{\rho_P}{R}\Big)^6}}\right] - \frac{3}{\theta_\tau}\int_{\rho_\tau}^{\rho_N} \frac{\theta(r,t)}{r}\,dr\right\}, \end{aligned} \tag{58}$$

that evaluated for $t = t_D$ allows the actual computation of z_0, which turns out to be bounded. If instead $\theta_\tau = \theta_D$ and then $\rho_\tau = \rho_D$, let us write $\ln(\rho_P/\rho_D) = \ln(\rho_P/\rho_N) + \ln(\rho_N/\rho_D)$ noting that

$$\ln\frac{\rho_N}{\rho_D} - \frac{1}{\theta_D}\int_{\rho_D}^{\rho_N} \frac{\theta(r,t)}{r}\,dr = \int_{\rho_D}^{\rho_N} \frac{1}{r}\Big(1 - \frac{\theta(r,t)}{\theta_D}\Big)\,dr\,. \tag{59}$$

By taking the expansion

$$\theta(r,t) = \theta_D + \frac{\partial \theta}{\partial r}\Big|_{r=\rho_D} (r-\rho_D) + o(r-\rho_D)\,,$$

where

$$\frac{\partial \theta}{\partial r}\Big|_{r=\rho_D} = -\frac{\rho_D^2}{\rho_N^2(\dot\rho_N - \omega_N)}\,,$$

as obtained by (50), we see that the integral in the right-hand side of (59) is bounded also for $t \to t_D^+$. So z_0 in (58) is still bounded. $\square$

Remark 6.1 *In order to have a solution with* $\omega_N < 0$, *and consequently* $p_C > p_E$, *for* $t > t_D$, *it is necessary that* $z_0 \le 0$. *The inequality* $z_0 \le 0$ *implies a constraint that can be made explicit from* (58). *If* $0 < \theta_\tau \le \theta_D$, *a sufficient condition for* $z_0 \le 0$ *is given by*

$$\begin{aligned} \frac{2\gamma}{R} &+ \psi(R) - \frac{4}{3}\eta_C \chi\Big[1 - \Big(\frac{\rho_P}{R}\Big)^3\Big] + \frac{1}{\nu(1-\nu)K}\frac{\chi}{3}(R-\rho_P)^2\Big(\frac{1}{2} + \frac{\rho_P}{R}\Big) \\ &- \frac{2}{\sqrt{3}}\tau_0 \ln\left[\Big(\frac{\rho_P}{\rho_\tau}\Big)^3 \frac{1+\sqrt{\frac{3}{2}}}{\Big(\frac{\rho_P}{R}\Big)^3 + \sqrt{\frac{1}{2} + \Big(\frac{\rho_P}{R}\Big)^6}}\right] \ge 0\,, \end{aligned} \tag{60}$$

where R, ρ_P, ρ_τ *are evaluated at* $t = t_D$. *If* $\theta_\tau \to 0$, *the above condition becomes*

$$\begin{aligned} \frac{2\gamma}{R} &+ \psi(R) - \frac{4}{3}\eta_C \chi\Big[1 - \Big(\frac{\rho_P}{R}\Big)^3\Big] + \frac{1}{\nu(1-\nu)K}\frac{\chi}{3}(R-\rho_P)^2\Big(\frac{1}{2} + \frac{\rho_P}{R}\Big) \\ &- \frac{2}{\sqrt{3}}\tau_0 \ln\left[\Big(\frac{\rho_P}{\rho_N}\Big)^3 \frac{1+\sqrt{\frac{3}{2}}}{\Big(\frac{\rho_P}{R}\Big)^3 + \sqrt{\frac{1}{2} + \Big(\frac{\rho_P}{R}\Big)^6}}\right] \ge 0\,, \end{aligned} \tag{61}$$

and it is also necessary.

Since the factor multiplying τ_0 *is positive, this constraint is actually limiting the choice of* γ *and* τ_0 *(if the viscosity and permeability terms have much less influence).*

Note that (61) implies $p_C(R_D, t_D) > p_E(R_D, t_D)$ as given by (44).

7 Analysis of system (47), (48), (56)

For simplicity, we confine to the case $\theta_\tau \to 0$. The system (47), (48), (56) must be studied for $t > t_D$. Eq. (47) is accompanied by the condition $R(t_D) = R_D$. The interfaces ρ_P, ρ_N are also known for $0 \le t \le t_D$, and by definition $\rho_D(t_D) = 0$. In the following we shall strengthen condition (61) by requiring

(a1) Inequality (61) is satisfied for all $R \ge R_D$ in the strict sense.

Let us rewrite the system (47), (48), (56) with the substitutions

$$X = \frac{1}{3}R^3\,, \quad Y_i = \frac{1}{3}\rho_i^3\,, \quad \Omega_N = \rho_N^2 \omega_N\,, \quad Z = \Omega_N / Y_D,\,,$$

where $i = P, N, D$. The advantage of introducing Z is just to emphasize that it is bounded and that terms like ZY_D^n with $n > 0$ vanish for $R \to R_D^+$, i.e., for $t \to t_D^+$. For $t > t_D$ we get

$$\dot{X} = \Omega_N + \chi(X - Y_P)\,, \qquad X(t_D) = \frac{1}{3}R_D^3 = X_D\,, \tag{62}$$

$$Y_D(t) = Y_N(t - \theta_D) + \int_{t-\theta_D}^{t} \Omega_N(s)\,ds\,, \tag{63}$$

$$\begin{aligned}
\frac{2\gamma}{(3X)^{1/3}} &= -\Psi(X) + \frac{4}{3}\eta_C \chi\Big(1 - \frac{Y_P}{X}\Big) - \frac{1}{\nu(1-\nu)K}\frac{\chi X^{2/3}}{2\cdot 3^{1/3}}\Big[1 - 3\Big(\frac{Y_P}{X}\Big)^{2/3} + 2\frac{Y_P}{X}\Big] \\
&- \ Z\left[\frac{4}{3}\eta_C\Big(1 - \frac{Y_D}{X}\Big) + \frac{1}{\nu(1-\nu)K}\frac{1}{3^{1/3}}Y_D^{2/3}\left(1 - \Big(\frac{Y_D}{X}\Big)^{1/3}\right)\right] \\
&+ \ \frac{2\sqrt{3}}{3}\tau_0\left[\ln\frac{X}{Y_N} + \ln\frac{1 + \sqrt{\frac{1}{2}\zeta^2 + 1}}{1 + \sqrt{\frac{1}{2}\Big(\frac{X}{Y_P}\zeta\Big)^2 + 1}}\right]\,,
\end{aligned} \tag{64}$$

where $\Psi(X) = \psi((3X)^{1/3})$ and

$$\zeta = \frac{1}{1 - \frac{\Omega_N}{\chi Y_P}}\,.$$

In the system (62)-(64) Y_P, Y_N are known functions of X. Moreover $\Omega_N(t) \equiv 0$ for $t_N \le t \le t_D$, and for $t > t_D$ it is looked for as a negative continuous function such that $Z(t_D) = 3\rho_N^3(t_D)z_0 = Z_0$. In the time interval $(t_D, t_D + \theta_D)$ the free term $Y_N(t - \theta_D)$ in (63) is known from the previous stage since R is known. As long as the constraint $\Omega_N \le 0$ is fulfilled, from (63) we have the inequality

$$Y_D(t) \le Y_N(t - \theta_D)\,, \qquad t > t_D\,. \tag{65}$$

We have the following:

Lemma 7.1 *Given* $0 < Y_D, Y_N, Y_P < X$*, the right-hand side of* (64) *is a decreasing function of* Ω_N *for* $\Omega_N < 0$*, which tends to* $+\infty$ *for* $\Omega_N \to -\infty$*. As long as* $X > X_D$*, under the assumption* **(a1)***, Eq.* (64) *provides a unique determination of* Ω_N *in* $(-\infty, 0)$*.*

Proof The first statement is trivial, although it requires some lengthy calculations. The second is a consequence of the just established monotonicity and of the fact that, thanks to **(a1)**, (64) can be satisfied only once when Ω_N ranges from 0 to $-\infty$. $\square$

On the basis of the preceding Lemma we can say that Ω_N can be expressed from (64) as a function of X, $Y_P(X)$, $Y_N(X)$ and Y_D (which is in turn a functional of Ω_N and X).

At this point we have to investigate the dependence of Y_P, Y_N over X, which has to be deduced from system (6)-(11), in which both t and R play the role of independent parameters (the actual time dependence is through $R(t)$). The following analysis refers to some fixed $t > t_D$ and R variable ($R > R_D$), so we will denote the oxygen concentration by $\sigma(r, R)$. We represent the oxygen absorption rate in the form

$$f(\sigma) = \tilde{f}(\sigma) + [f]H(\sigma - \sigma_P)\,, \tag{66}$$

where $\tilde{f}(\sigma)$ is continuous, with a bounded continuous derivative on both sides of σ_P, H is the Heaviside function, and $[f]$ is the jump of f across σ_P:

$$[f] = (m-1)\tilde{f}(\sigma_P)\,. \tag{67}$$

Integrating the oxygen diffusion-consumption equation over (ρ_N, r), with the condition $\sigma_r(\rho_N, R) = 0$, we obtain

$$\frac{\partial \sigma}{\partial r} = \frac{1}{r^2}\int_{\rho_N}^{r} r'^2 \tilde{f}(\sigma)\, dr' + [f]\frac{\bar{r}_P^3 - \rho_P^3}{3r^2}\,, \tag{68}$$

where $\bar{r}_P = \max(r, \rho_P)$ is a Lipschitz continuous function of r. A further integration over the interval (r, R) with the condition $\sigma|_{r=R} = \sigma^*$ yields

$$\begin{aligned} \sigma^* - \sigma(r,R) \;&=\; \int_{\rho_N}^{R}\Big(\frac{1}{\max(r,r')} - \frac{1}{R}\Big) r'^2 \tilde{f}(\sigma)\, dr' \\ &+\;\; [f]\left[\frac{1}{6}\Big(R^2 - \bar{r}_P^2\Big) - \frac{1}{3}\rho_P^3\left(\frac{1}{\bar{r}_P} - \frac{1}{R}\right)\right]. \end{aligned} \tag{69}$$

On the basis of (69) we are able to show the boundedness of the derivatives

$$\frac{\partial \sigma}{\partial R} = \Sigma(r,R)\,, \qquad \frac{\partial \rho_i}{\partial R} = P_i(R)\,, \quad i = P, N\,.$$

Lemma 7.2 *Under the condition*

$$R^2\Big[\frac{1}{6} - \frac{1}{2}\Big(\frac{\rho_N}{R}\Big)^2 + \frac{1}{3}\Big(\frac{\rho_N}{R}\Big)^3\Big] \sup_{\sigma\in(\sigma_N,\sigma^*)} |\tilde{f}'| < 1 \tag{70}$$

for all $R > R_D$, and if $[f]$ is sufficiently small, the quantities Σ and P_i are a-priori bounded.

Proof By differentiating (69) with respect to R and recalling that

$$\frac{\partial \bar{r}_P}{\partial R} = 0 \;\text{ if }\; r > \rho_P\,, \quad \frac{\partial \bar{r}_P}{\partial R} = P_P \;\text{ if }\; r \le \rho_P\,,$$

i.e., $\partial\bar r_P/\partial R = P_P H(\rho_P - r)$, we obtain

$$\begin{aligned} -\Sigma = {} & \frac{1}{R^2}\int_{\rho_N}^{R} r'^2 \tilde f(\sigma)\,dr' + \int_{\rho_N}^{R}\Big(\frac{1}{\max(r,r')} - \frac{1}{R}\Big) r'^2 \tilde f'(\sigma)\Sigma\,dr' \\ & - \Big(\frac{1}{r} - \frac{1}{R}\Big) P_N \rho_N^2 \tilde f(\sigma_N) + [f]\Big\{\frac{1}{3}R\Big[1 - \Big(\frac{\rho_P}{R}\Big)^3\Big] - \rho_P^2 P_P\Big(\frac{1}{\bar r_P} - \frac{1}{R}\Big)\Big\}\,. \end{aligned} \tag{71}$$

Thus we conclude that Σ is a continuous function of r.

Now, differentiating with respect to R the identities

$$\sigma(\rho_N, R) = \sigma_N\,, \qquad \sigma(\rho_P, R) = \sigma_P\,,$$

and making use of (68), we get the equalities

$$\Sigma|_{r=\rho_N} = 0\,, \tag{72}$$

$$P_P \frac{1}{\rho_P^2}\int_{\rho_N}^{\rho_P} r^2 \tilde f(\sigma)\,dr + \Sigma|_{r=\rho_P} = 0\,. \tag{73}$$

After some algebra, system (72)-(73) can be put in the form

$$P_P \frac{1}{\rho_P^2}\int_{\rho_N}^{\rho_P} r^2 \tilde f(\sigma)\,dr - \Big(\frac{1}{\rho_N} - \frac{1}{\rho_P}\Big) P_N \rho_N^2 \tilde f(\sigma_N) = \int_{\rho_N}^{\rho_P}\Big(\frac{1}{\rho_P} - \frac{1}{r}\Big) r^2 \tilde f'(\sigma)\Sigma\,dr\,, \tag{74}$$

$$\begin{aligned} & P_P\,[f]\rho_P^2\Big(\frac{1}{\rho_P} - \frac{1}{R}\Big) + \Big(\frac{1}{\rho_N} - \frac{1}{R}\Big) P_N \rho_N^2 \tilde f(\sigma_N) \\ & = \frac{1}{R^2}\int_{\rho_N}^{R} r^2 \tilde f(\sigma)\,dr + \int_{\rho_N}^{R}\Big(\frac{1}{r} - \frac{1}{R}\Big) r^2 \tilde f'(\sigma)\Sigma\,dr + [f]\frac{1}{3}R\Big[1 - \Big(\frac{\rho_P}{R}\Big)^3\Big]\,, \end{aligned} \tag{75}$$

which can be regarded as a linear algebraic system in P_P,P_N, with determinant $\rho_N^2 \tilde f(\sigma_N) D^*$, where

$$D^* = \frac{1}{\rho_P^2}\Big(\frac{1}{\rho_N} - \frac{1}{R}\Big)\int_{\rho_N}^{\rho_P} r^2 \tilde f(\sigma)\,dr + [f]\rho_P^2\Big(\frac{1}{\rho_P} - \frac{1}{R}\Big)\Big(\frac{1}{\rho_N} - \frac{1}{\rho_P}\Big) > 0\,. \tag{76}$$

The triple (P_P, P_N, Σ) has to be derived from the system (71), (74), (75). We remark that, comparing (68) and (71) for $r = R$, we see that the identity

$$\frac{\partial\sigma}{\partial r}\Big|_{r=R} + \Sigma|_{r=R} = 0$$

is satisfied.

The explicit expressions of P_P, P_N in terms of known functions of R and of integrals of Σ are the following

$$\begin{aligned} P_P = {} & \frac{1}{D^*}\Big(\frac{1}{\rho_N} - \frac{1}{\rho_P}\Big)\Big\{\frac{1}{R^2}\int_{\rho_N}^{R} r^2 \tilde f(\sigma)\,dr + [f]\frac{1}{3}R\Big[1 - \Big(\frac{\rho_P}{R}\Big)^3\Big]\Big\} + \frac{1}{D^*}\Big[\Big(\frac{1}{\rho_N} - \frac{1}{R}\Big) \\ & \times \int_{\rho_N}^{\rho_P}\Big(\frac{1}{\rho_P} - \frac{1}{r}\Big) r^2 \tilde f'(\sigma)\Sigma\,dr + \Big(\frac{1}{\rho_N} - \frac{1}{\rho_P}\Big)\int_{\rho_N}^{R}\Big(\frac{1}{r} - \frac{1}{R}\Big) r^2 \tilde f'(\sigma)\Sigma\,dr\Big]\,, \end{aligned} \tag{77}$$

$$\begin{aligned} P_N\rho_N^2\tilde{f}(\sigma_N) &= \frac{1}{D^*}\frac{1}{\rho_P^2}\int_{\rho_N}^{\rho_P} r^2\tilde{f}(\sigma)\,dr\Big\{\frac{1}{R^2}\int_{\rho_N}^{R} r^2\tilde{f}(\sigma)\,dr + [f]\frac{1}{3}R\Big[1-\Big(\frac{\rho_P}{R}\Big)^3\Big]\Big\} \\ &+ \frac{1}{D^*}\Big[\frac{1}{\rho_P^2}\int_{\rho_N}^{\rho_P} r^2\tilde{f}(\sigma)\,dr\int_{\rho_N}^{R}\Big(\frac{1}{r}-\frac{1}{R}\Big)r^2\tilde{f}'(\sigma)\Sigma\,dr \\ &- [f]\rho_P^2\Big(\frac{1}{\rho_P}-\frac{1}{R}\Big)\int_{\rho_N}^{\rho_P}\Big(\frac{1}{\rho_P}-\frac{1}{r}\Big)r^2\tilde{f}'(\sigma)\Sigma\,dr\Big]\,. \end{aligned} \tag{78}$$

With the help of (77)-(78), from (71) we deduce the following integral equation for $\Sigma(r,R)$:

$$\begin{aligned} -\Sigma &= \frac{1}{R^2}\int_{\rho_N}^{R} r'^2\tilde{f}(\sigma)\,dr' + \int_{\rho_N}^{R}\Big(\frac{1}{\max(r,r')}-\frac{1}{R}\Big)r'^2\tilde{f}'(\sigma)\Sigma\,dr' + [f]\frac{1}{3}R\Big[1-\Big(\frac{\rho_P}{R}\Big)^3\Big] \\ &- \Big(\frac{1}{r}-\frac{1}{R}\Big)\frac{1}{D^*}\frac{1}{\rho_P^2}\int_{\rho_N}^{\rho_P} r^2\tilde{f}(\sigma)\,dr\Big\{\frac{1}{R^2}\int_{\rho_N}^{R} r^2\tilde{f}(\sigma)\,dr + [f]\frac{1}{3}R\Big[1-\Big(\frac{\rho_P}{R}\Big)^3\Big]\Big\} \\ &- \Big(\frac{1}{r}-\frac{1}{R}\Big)\frac{1}{D^*}\Big[\frac{1}{\rho_P^2}\int_{\rho_N}^{\rho_P} r^2\tilde{f}(\sigma)\,dr\int_{\rho_N}^{R}\Big(\frac{1}{r'}-\frac{1}{R}\Big)r'^2\tilde{f}'(\sigma)\Sigma\,dr' \\ &- [f]\rho_P^2\Big(\frac{1}{\rho_P}-\frac{1}{R}\Big)\int_{\rho_N}^{\rho_P}\Big(\frac{1}{\rho_P}-\frac{1}{r'}\Big)r'^2\tilde{f}'(\sigma)\Sigma\,dr'\Big] \\ &- [f]\rho_P^2\Big(\frac{1}{\bar{r}_P}-\frac{1}{R}\Big)\frac{1}{D^*}\Big(\frac{1}{\rho_N}-\frac{1}{\rho_P}\Big)\Big\{\frac{1}{R^2}\int_{\rho_N}^{R} r^2\tilde{f}(\sigma)\,dr + [f]\frac{1}{3}R\Big[1-\Big(\frac{\rho_P}{R}\Big)^3\Big]\Big\} \\ &- [f]\rho_P^2\Big(\frac{1}{\bar{r}_P}-\frac{1}{R}\Big)\frac{1}{D^*}\Big[\Big(\frac{1}{\rho_N}-\frac{1}{R}\Big)\int_{\rho_N}^{\rho_P}\Big(\frac{1}{\rho_P}-\frac{1}{r'}\Big)r'^2\tilde{f}'(\sigma)\Sigma\,dr' \\ &+ \Big(\frac{1}{\rho_N}-\frac{1}{\rho_P}\Big)\int_{\rho_N}^{R}\Big(\frac{1}{r'}-\frac{1}{R}\Big)r'^2\tilde{f}'(\sigma)\Sigma\,dr'\Big]\,. \end{aligned} \tag{79}$$

The structure of this equation is of the type

$$\Sigma(r,R) + \int_{\rho_N}^{R} K(r,r',R)\Sigma(r',R)\,dr' = M(r,R)\,, \tag{80}$$

where K, M are continuous and bounded for $\rho_N \le r \le R$, and $R \in (R_D, R_{max})$ for some fixed R_{max}. Thus, for each R we are dealing with a Fredholm equation of the second kind.

The kernel $K(r,r',R)$ has the expression:

$$K(r,r',R) = \hat{K}(r,r',R)r'^2\tilde{f}'(\sigma(r',R))\,,$$

with

$$\begin{aligned} \hat{K}(r,r',R) &= \frac{1}{\max(r,r')} - \frac{1}{R} - \Big(\frac{1}{r}-\frac{1}{R}\Big)\frac{1}{D^*}\frac{1}{\rho_P^2}\Big(\frac{1}{r'}-\frac{1}{R}\Big)\int_{\rho_N}^{\rho_P} r^2\tilde{f}(\sigma)\,dr \\ &- [f]\rho_P^2\Big\{\Big(\frac{1}{\rho_P}-\frac{1}{R}\Big)\Big(\frac{1}{\rho_P}-\frac{1}{r'}\Big) + \Big(\frac{1}{\bar{r}_P}-\frac{1}{R}\Big)\frac{1}{D^*}\Big[\Big(\frac{1}{\rho_N}-\frac{1}{R}\Big) \\ &\times \Big(\frac{1}{\rho_P}-\frac{1}{r'}\Big)H(\rho_P-r') + \Big(\frac{1}{\rho_N}-\frac{1}{\rho_P}\Big)\Big(\frac{1}{r'}-\frac{1}{R}\Big)\Big]\Big\}\,. \end{aligned} \tag{81}$$

Neglecting $[f]$ in (81) we define a reduced kernel

$$\hat{K}_0(r,r',R) = \Big(\frac{1}{\max(r,r')} - \frac{1}{R}\Big)\Big[1 - \Big(\frac{1}{\min(r,r')} - \frac{1}{R}\Big)\frac{1}{\hat{D}^*}\int_{\rho_N}^{\rho_P} (\frac{r}{\rho_P})^2 \tilde{f}(\sigma)\, dr\Big] ,$$

where $\hat{D}^*$ is obtained from (76) setting $[f] = 0$. $\hat{K}_0$ is positive since

$$\Big(\frac{1}{\min(r,r')} - \frac{1}{R}\Big)\frac{1}{\hat{D}^*}\int_{\rho_N}^{\rho_P} (\frac{r}{\rho_P})^2 \tilde{f}(\sigma)\, dr \le \Big(\frac{1}{\rho_N} - \frac{1}{R}\Big)\frac{1}{\hat{D}^*}\int_{\rho_N}^{\rho_P} (\frac{r}{\rho_P})^2 \tilde{f}(\sigma)\, dr < 1$$

and the latter inequality holds in view of (76). Moreover the inequality

$$\hat{K}_0(r,r',R) < \frac{1}{\rho_N} - \frac{1}{R} \tag{82}$$

can be easily seen. If we impose that $\hat{K}_0 r'^2 \tilde{f}'$ has L^1 norm (w.r.t. r') less than 1, i.e. condition (70), then, for $[f]$ sufficiently small, the kernel K has the same property and Eq. (80) has a unique solution in the space of continuous functions. An a priori bound for this solution can be found, depending on $(1 - \|K\|_1)^{-1}$, where $\|K\|_1 = \sup_{(r,R)} \|K(r,\cdot,R)\|_{L^1}$.

Under the choice

$$\tilde{f}(\sigma) = \frac{1}{\phi^2}\frac{\sigma}{1+\sigma/H} ,$$

we get $|\tilde{f}'| < 1/\phi^2$, where ϕ is a length.

Once an estimate has been obtained for Σ, going back to (77) and (78), bounds on P_P, P_N follow. $\square$

Remark 7.1 *Using the* L^2 *in place of the* L^1 *norm of* $\hat{K}_0 r'^2 \tilde{f}'$*, a condition milder than* (70) *can be obtained.*

We now proceed supposing that bounds on P_P, P_N are known. Since

$$\frac{\partial Y_i}{\partial X} = P_i \left(\frac{Y_i}{X}\right)^{2/3} , \qquad i = P, N , \tag{83}$$

it turns out that Y_P, Y_N are uniformly Lipschitz continuous functions of X in a compact set such that $X \ge X_D$. We keep writing Y_P, Y_N to denote both the functions of X and the functions of t through $X(t)$. As functions of t, their Lipschitz norm depends also on $\sup|\dot{X}|$ in a given interval $[t_D, T]$. The function $Y_D(t)$ is also Lipschitz continuous with a norm estimated by the sum of the Lipschitz norm of $Y_N(t)$ and of the product $\theta_D\|\Omega_N\|$, with $\|\cdot\|$ denoting the sup-norm in $[t_D, T]$.

Remark 7.2 *The difference* $\dot{Y}_N - \Omega_N = \rho_N^2(\dot{\rho}_N - \omega_N)$ *equals* $\frac{1}{4\pi}$ *times the volume feeding rate of the necrotic core. At the beginning of stage IV we have* $\omega_N = 0$ *and* $\dot{\rho}_N > 0$*, while at a possible steady state we will have* $\dot{\rho}_N = 0$ *and necessarily* $\omega_N < 0$ *as, thanks to* (62)*, the two speeds cannot vanish simultaneously. We can verify that* *the difference* $\dot{Y}_N - \Omega_N$ *is positive and bounded away from zero for any* t*. Indeed, recalling* (83) *and* (62)*, the requirement* $\dot{Y}_N - \Omega_N \geq \mu$ *for some* $\mu > 0$ *is equivalent to*

$$\chi(X - Y_P) P_N \Big(\frac{Y_N}{X}\Big)^{2/3} > \mu + \Omega_N \Big[1 - P_N \Big(\frac{Y_N}{X}\Big)^{2/3}\Big] , \tag{84}$$

which is automatically satisfied for $\Omega_N < 0$ *if*

$$P_N \Big(\frac{Y_N}{X}\Big)^{2/3} < 1 . \tag{85}$$

Numerical simulations suggested that, for $X \geq X_D$*, inequality* (85) *holds true for the solution of the diffusion problem* (6)-(11)*.*

Now we want to prove an existence result for system (62)-(64). Besides **(a1)** that, rewritten in the new variables, becomes

$$\frac{2\gamma}{(3X)^{1/3}} > -\Psi(X) + \frac{4}{3}\eta_C \chi \Big(1 - \frac{Y_P}{X}\Big) - \frac{1}{\nu(1-\nu)K} \frac{\chi X^{2/3}}{2 \cdot 3^{1/3}} \Big[1 - 3\Big(\frac{Y_P}{X}\Big)^{2/3} + 2\frac{Y_P}{X}\Big]$$

$$+ \quad \frac{2\sqrt{3}}{3}\tau_0 \Big[\ln \frac{X}{Y_N} + \ln \frac{1 + \sqrt{\frac{1}{2}\zeta^2 + 1}}{1 + \sqrt{\frac{1}{2}\Big(\frac{X}{Y_P}\zeta\Big)^2 + 1}}\Big] , \qquad X \geq X_D , \tag{86}$$

we impose

(a2) the function Ψ, besides being nonnegative and nondecreasing, is Lipschitz continuous.

Condition (86) implies that $\Omega_N = 0$ is never a solution of (64) when $X > X_D$, $Y_D > 0$. We will prove the following:

Theorem 7.1 *Under the assumptions* **(a1)**-**(a2)** *and of Lemma 7.2, system* (62)-(64) *has a unique solution in some time interval* $[t_D, T]$*,* $t_D < T \leq t_D + \theta_D$*.*

Proof We still denote by Z_0 the limit of Ω_N / Y_D for $t \to t_D^+$. Assumption **(a1)** implies $Z_0 < 0$, and we look for $\Omega_N(t)$ in the form

$$\Omega_N(t) = Z_0 Y_D(t)[1 + \xi(t)] \tag{87}$$

with

$$\xi(t_D) = 0 , \qquad 1 + \xi(t) \geq 0 . \tag{88}$$

Accordingly, (64) is rewritten with the factor Z replaced by $Z_0[1 + \xi(t)]$ and

$$\zeta = \Big[1 - \frac{Z_0 Y_D (1 + \xi)}{\chi Y_P}\Big]^{-1} . \tag{89}$$

Our new unknown is $\xi(t)$, and we look for it in the following compact set

$$\Lambda(T,\Xi,L) \;=\; \big\{\xi \in \mathcal{C}[t_D,T],\ t_D < T \leq t_D+\theta_D \,:\, \xi(t_D)=0,\, 0\leq 1+\xi \leq \Xi\,, \\ \sup_{t_1,t_2\in[t_D,T]} \Big|\frac{\xi(t_1)-\xi(t_2)}{t_1-t_2}\Big| \leq L\big\} \tag{90}$$

for some $\Xi > 1$ and $L > 0$ to be chosen together with T. We set up a fixed point argument. For a given $\xi \in \Lambda$ we consider the equations

$$\dot{X} = Z_0 Y_D(t)[1+\xi(t)] + \chi[X(t)-Y_P(t)]\,, \qquad t > t_D \tag{91}$$

$$Y_D(t) = Y_N(t-\theta_D) + \int_{t_D}^{t} Z_0 Y_D(s)[1+\xi(s)]\,ds\,, \qquad t > t_D\,, \tag{92}$$

derived from (62)-(63) and we compute the functions X, Y_D. We point out that when $t \in (t_D, t_D+\theta_D]$ the lower limit of the integral in (63) reduces to t_D, since $\Omega_N(t)=0$ for $t \leq t_D$, and that the function $Y_N(t-\theta_D)$ is a known positive, increasing function of order $(t-t_D)^3$.

Owing to (92), $Y_D(t) < Y_N(t-\theta_D)$ for $t > t_D$. We can force $X(t)$ to be increasing if we impose that

$$|Z_0| Y_N(t-\theta_D)[1+\xi(t)] < \chi \inf_{X\geq X_D}(X-Y_P) = V^*\,.$$

Remembering that $Y_N(t_D-\theta_D)=0$ (which is nothing but the definition of t_D) we can find some $T_D \in (t_D, t_D+\theta_D]$ such that

$$\Xi^* = \frac{V^*}{|Z_0| Y_N(T_D-\theta_D)} > 1\,. \tag{93}$$

Therefore, we take $\Xi \geq \Xi^*$ and, for the moment, $T \leq T_D$ in (90). For X we have the trivial estimate

$$X_D \leq X \leq X_D \exp\left[\chi(T-t_D)\right]. \tag{94}$$

Since ξ has been given in Λ, (92) is actually an integral equation of Volterra type. We can see that $Y_D(t)$ is positive like the free term in (92), and that, irrespective of the choice of ξ, for $t-t_D$ small and positive it behaves like $Y_N(t-\theta_D)$, which is $O(t-t_D)^3$. Moreover, it is easy to obtain a bound for $\dot{Y}_D(t)$ of the type

$$\|\dot{Y}_D\| \leq A + B\,\Xi \tag{95}$$

for some positive constants A, B, uniformly with respect to the choice of ξ in Λ.

At this point we go back to (64), where $X(t)$, $Y_D(t)$ are the functions just found and, in view of Lemma 7.1, we know that from it we can deduce a new determination of our unknown, that we call $\tilde{\xi}(t)$. Thus we have defined the mapping

$$\xi \to \tilde{\xi}\,.$$

In order to study such a mapping it is convenient to give a new form to (64). To this end, let us define

$$\begin{aligned} M(X) \;=\; & \frac{2\gamma}{(3X)^{1/3}} + \Psi(X) - \frac{4}{3}\eta_C \chi\Big(1 - \frac{Y_P}{X}\Big) + \frac{1}{\nu(1-\nu)K}\frac{\chi X^{2/3}}{2\cdot 3^{1/3}} h(X) \\ - \;\; & \frac{2\sqrt{3}}{3}\tau_0 \ln\frac{X}{Y_N}\,, \end{aligned} \tag{96}$$

with

$$h(X) = 1 - 3\Big(\frac{Y_P}{X}\Big)^{2/3} + 2\frac{Y_P}{X}\,,$$

and introduce

$$g(X,\zeta) = \ln\frac{1 + \sqrt{\frac{1}{2}\zeta^2 + 1}}{1 + \sqrt{\frac{1}{2}\Big(\frac{X}{Y_P}\zeta\Big)^2 + 1}}\,. \tag{97}$$

Then (64) takes the form

$$\begin{aligned} M(X) \;=\; & -Z\left[\frac{4}{3}\eta_C\Big(1 - \frac{Y_D}{X}\Big) + \frac{1}{\nu(1-\nu)K}\frac{1}{3^{1/3}}Y_D^{2/3}\left(1 - \Big(\frac{Y_D}{X}\Big)^{1/3}\right)\right] \\ + \;\; & \frac{2\sqrt{3}}{3}\tau_0 \ln g(X,\zeta)\,, \end{aligned} \tag{98}$$

which, for $X \to X_D^+$, provides

$$-Z_0 \cdot \frac{4}{3}\eta_C = M(X_D) - \frac{2\sqrt{3}}{3}\tau_0 \ln g(X_D,1)\,. \tag{99}$$

Putting $Z = Z_0(1+\xi)$ in (98) and using (99) we have

$$\begin{aligned} - \;\; & Z_0\xi\left[\frac{4}{3}\eta_C\Big(1 - \frac{Y_D}{X}\Big) + \frac{1}{\nu(1-\nu)K}\frac{1}{3^{1/3}}Y_D^{2/3}\left(1 - \Big(\frac{Y_D}{X}\Big)^{1/3}\right)\right] \\ - \;\; & Z_0\left[-\frac{4}{3}\eta_C\frac{Y_D}{X} + \frac{1}{\nu(1-\nu)K}\frac{1}{3^{1/3}}Y_D^{2/3}\left(1 - \Big(\frac{Y_D}{X}\Big)^{1/3}\right)\right] \\ + \;\; & \frac{2\sqrt{3}}{3}\tau_0[\ln g(X,\zeta) - \ln g(X_D,1)] = M(X) - M(X_D)\,, \end{aligned}$$

and, dividing by $-Z_0\frac{4}{3}\eta_C$, we obtain

$$\begin{aligned} & \xi\;\;[1 + N(Y_D,X)] + N(Y_D,X) + \frac{2\sqrt{3}}{3}\tau_0\frac{\ln g(X,\zeta) - \ln g(X_D,1)}{M(X_D) - \frac{2\sqrt{3}}{3}\tau_0\ln g(X_D,1)} \\ & = \frac{M(X) - M(X_D)}{M(X_D) - \frac{2\sqrt{3}}{3}\tau_0\ln g(X_D,1)}\,, \end{aligned} \tag{100}$$

where

$$N(Y_D, X) = -\frac{Y_D}{X} + \frac{1}{\nu(1-\nu)K}\frac{1}{3^{1/3}}Y_D^{2/3}\left(1-\left(\frac{Y_D}{X}\right)^{1/3}\right), \tag{101}$$

and ζ is given by (89). Equation (100) is the desired new form of (64) on which the mapping $\xi \to \tilde{\xi}$ is based.

From (91) and (95), and using Lemma 7.2, we deduce that for any $\xi \in \Lambda$ the functions X, Y_P, Y_N, Y_D have a Lipschitz norm which is bounded by a constant that depends on Ξ only. In addition, we remark that $Y_D^{1/3}$ is Lipschitz and $O(t-t_D)$, as it can be inferred from (63), where the integral of Ω_N is $O(t-t_D)^4$ and $Y_N(t-\theta_D) = O(t-t_D)^3$. The Lipschitz norm of Y_D^3 has also a bound dependent on Ξ only. The same property is transferred to $Y_D^{2/3}$ appearing in (101). Thus, from (100), it is easy to infer that $\tilde{\xi}$ is Lipschitz with a norm bounded by $\hat{L}(\Xi)$. At this point in (90) we choose $\Xi = \Xi^*$ and we take $L = \hat{L}(\Xi^*)$. We conclude that the function $\tilde{\xi}$ has the following properties:

(p1) $\tilde{\xi}(t_D) = 0$;

(p2) $\tilde{\xi}$ has a Lipschitz norm $L_{\tilde{\xi}} \le L$;

(p3) $1 + \tilde{\xi}(t)$ cannot vanish for $t > t_D$, owing to (86), i.e., to assumption **(a1).**

Thanks to **(p2)**, **(p3)**, we have

$$0 < 1 + \tilde{\xi}(t) \le 1 + L(t - t_D). \tag{102}$$

Therefore, if we define T^* so that

$$1 + L(T^* - t_D) \le \Xi^*, \tag{103}$$

and we take $T \le \min(T_D, T^*)$, then we can say that $\tilde{\xi} \in \Lambda(T, \Xi, L)$ as well.

Now we prove that the mapping $\xi \to \tilde{\xi}$ is a contraction. To this aim we estimate the difference $\delta\tilde{\xi}$ corresponding to the difference $\delta\xi$ of two functions ξ_1, ξ_2 taken in Λ. It is easy to establish the following inequalities (remember that $\delta Y_N(t-\theta_D) \equiv 0$):

$$\|\delta Y_D\|_t \le A \int_{t_D}^{t} \max[Y_D^{(1)}(s), Y_D^{(2)}(s)] \|\delta\xi\|_s \, ds, \tag{104}$$

$$\|\delta X\|_t \le A_1 \int_{t_D}^{t} \|\delta X\|_s \, ds + B_1 \int_{t_D}^{t} \|\delta\xi\|_s \, ds, \tag{105}$$

where δ denotes variation, $\|\cdot\|_s$ is the sup-norm in the interval (t_D, s), and $Y_D^{(j)}$, $j = 1, 2$, denote the two determinations of Y_D under consideration. A, A_1, B_1 are positive constants independent of the choice of the two functions ξ_1, ξ_2. All constants that will be introduced in the sequel are meant to have the same property. From (105) we deduce that

$$\|\delta X\|_t \le C_1 \int_{t_D}^{t} \|\delta\xi\|_s \, ds, \tag{106}$$

and therefore

$$\|\delta Y_D\|_t \le C_2(t-t_D)\int_{t_D}^{t} \|\delta\xi\|_s\, ds\,. \tag{107}$$

We remark that the derivatives dM/dX, $\partial g/\partial X$, $\partial g/\partial\zeta$, and $\partial N/\partial X$ are bounded in the range of interest, while $\partial N/\partial Y_D$ is not, owing to the term containing $Y_D^{2/3}$ (remember that $Y_D^{-1/3} \approx (t-t_D)^{-1}$).

In order to estimate $\delta Y_D^{2/3}$ we not only need (107) but also a lower estimate for Y_D, which can be deduced directly from (63):

$$Y_D(t) > Y_N(t-\theta_D) - |Z_0|\|Y_D\|_t\,\Xi^*(t-t_D)\,.$$

The inequality makes sense for $t-t_D$ small enough, since the negative term is one order of magnitude smaller than $Y_N(t-\theta_D)$ (remember that $\|Y_D\|_t$ has the same order as $Y_N(t-\theta_D)$). Reducing T, the above inequality can be written

$$Y_D(t) > bY_N(t-\theta_D)\,,$$

for some $b \in (0,1)$. Thus, if we take a pair of functions ξ_1, ξ_2 in Λ and consider the corresponding functions $Y_D^{(1)}$, $Y_D^{(2)}$, recalling that, irrespective of ξ, for $t-t_D$ small $Y_D(t)$ behaves like $Y_N(t-\theta_D)$ which is $O(t-t_D)^3$, the ratio

$$\frac{\max(Y_D^{(1)}(t), Y_D^{(2)}(t))}{\min(Y_D^{(1)}(t), Y_D^{(2)}(t))}$$

is bounded by a constant α which is close to 1 as we like, provided $T-t_D$ is small enough.

From this analysis we conclude that

$$\|\delta Y_D^{2/3}\| \le C_3\int_{t_D}^{t} \|\delta\xi\|_s\, ds\,, \tag{108}$$

where, to simplify notations, from now on we write $\|\cdot\|$ meaning $\|\cdot\|_t$. In the following we set $\|Y_D\| = \max_{i=1,2}\|Y_D^{(i)}\|$ and similarly for the norms of functions corresponding to either ξ_1 or ξ_2. Thus,

$$\begin{aligned}\|\delta N\| \le\ & \frac{\|\delta Y_D\|}{X_D} + \frac{\|Y_D\|\|\delta X\|}{X_D^2} + \frac{1}{\nu(1-\nu)K}\frac{3^{2/3}}{4\eta_C}\left[C_3\int_{t_D}^{t}\|\delta\xi\|_s\, ds + \frac{\|\delta Y_D\|}{X_D^{1/3}}\right.\\ &+ \left.\frac{\|Y_D\|}{X_D^{2/3}}\|\delta X\|\right] \le C_4\|Y_D\|\|\delta Y_D\| + C_5\|\delta X\| + C_6\int_{t_D}^{t}\|\delta\xi\|_s\, ds\,. \end{aligned} \tag{109}$$

Moreover, writing

$$\zeta(X, Y_D, \tilde{\xi}) = \left[1 - \frac{Z_0 Y_D(1+\tilde{\xi})}{\chi Y_P}\right]^{-1},$$

and knowing that $\alpha\zeta \leq 1$ for $t - t_D$ small enough, we find

$$\|\delta\zeta\| \leq \frac{|Z_0|\Xi}{\chi Y_P(t_D)}\left(\|\frac{\partial Y_P}{\partial X}\|\|Y_D\|\|\delta X\| + \frac{1}{Y_P(t_D)}\|\delta Y_D\|\right) + \frac{|Z_0|\|Y_D\|}{\chi Y_P(t_D)}\|\delta\tilde{\xi}\|\,. \tag{110}$$

At this point, from (100) we deduce

$$\|\delta\tilde{\xi}\| \leq \Xi\|\delta N\| + \frac{1}{M(X_D) + \frac{2\sqrt{3}}{3}\tau_0 \ln g(X_D,1)}\left\{\frac{2\sqrt{3}}{3}\tau_0\left[\|\frac{\partial g}{\partial X}\|\|\delta X\| + \|\frac{\partial g}{\partial \zeta}\|\|\delta\zeta\|\right] + \|\frac{dM}{dX}\|\|\delta X\|\right\}, \tag{111}$$

and exploiting (109), (110) together with (106), (107) we obtain

$$\|\delta\tilde{\xi}\| \leq \frac{\frac{2\sqrt{3}}{3}\tau_0}{M(X_D) + \frac{2\sqrt{3}}{3}\tau_0 \ln g(X_D,1)}\|\frac{\partial g}{\partial \zeta}\|\frac{|Z_0|\|Y_D\|}{\chi Y_P(t_D)}\|\delta\tilde{\xi}\| + C_7\int_{t_D}^{t}\|\delta\xi\|_s\,ds\,.$$

Hence, recalling that $\|Y_D\|$ is infinitesimal with $t - t_D$, we conclude that by suitably reducing the time T we can make the mapping $\xi \to \tilde{\xi}$ a contraction. Existence and uniqueness follow from the Banach fixed point theorem. ☐

Using in combination the Shauder's theorem, exploiting the compactness of Λ, continuation of the solution is readily obtained.

8 Stationary state

At a possible steady state we have $\dot{R} = 0$, all the interfaces are stationary, and the cell velocity and the pressure fields are time independent. Thus, from Eq. (47) we obtain

$$\omega_N = -\frac{\chi}{3\rho_N^2}\left(R^3 - \rho_P^3\right). \tag{112}$$

Moreover, taking into account (112), from Eqs. (48) and (51) we have

$$\rho_D^3 = \rho_N^3 - \chi\theta_D(R^3 - \rho_P^3)\,, \tag{113}$$

$$\rho_\tau^3 = \rho_N^3 - \chi\theta_\tau(R^3 - \rho_P^3)\,, \tag{114}$$

and from (50)

$$\theta(r) = \frac{\rho_N^3 - r^3}{\chi(R^3 - \rho_P^3)}\,, \qquad \rho_D \leq r \leq \rho_N\,. \tag{115}$$

The equation (53) for the continuity of normal stress at $r = \rho_D$, in view of (112) and (115), becomes

$$
\begin{aligned}
2\gamma + R\psi(R) = {} & \frac{4}{3}\eta_C \chi R \frac{R^3 - \rho_P^3}{\rho_D^3} + \frac{1}{\nu(1-\nu)K}\frac{\chi R^3}{3}\left\{\frac{R}{\rho_D}\left[1 - \left(\frac{\rho_P}{R}\right)^3\right] - \frac{3}{2}\left[1 - \left(\frac{\rho_P}{R}\right)^2\right]\right\} \\
& + \frac{2}{\sqrt{3}}\tau_0 R \Bigg\{ \ln\left(\frac{\rho_p}{\rho_\tau}\right)^3 \frac{\left(\frac{R}{\rho_P}\right)^3 + \sqrt{\frac{1}{2} + \left(\frac{R}{\rho_P}\right)^6}}{1 + \sqrt{\frac{3}{2}}} \\
& - \frac{3\rho_N^3}{\theta_\tau \chi (R^3 - \rho_P^3)}\left[\ln\frac{\rho_N}{\rho_\tau} - \frac{1}{3}\left(1 - \left(\frac{\rho_\tau}{\rho_N}\right)^3\right)\right]\Bigg\}, \qquad (116)
\end{aligned}
$$

where ρ_D and ρ_τ are given by (113) and (114). Since ρ_P and ρ_N are functions of R after the solution of Problem (6)-(11), the above equation determines the value of R at the equilibrium.

From (113) it is easy to see that ρ_D vanishes at a certain value, R_a, of the radius R. Therefore, the right-hand-side of Eq. (116) tends to $+\infty$ for $R \to R_a^+$. The presence of a vertical asymptote at $R = R_a$ imposes a lower bound to the possible values of R at the steady state, which is independent of the values of γ, τ_0, η_C and K, and only depends on χ, θ_D and the parameters of problem (6)-(11). As θ_D decreases, from (113) we also see that R_a approaches R_N and, for θ_D small, $\rho_D \simeq \rho_N$, namely, the whole necrotic region will be liquid as expected. If $\theta_D \to \infty$, then $R_a \to \infty$.

It is possible to show that the right-hand-side of Eq. (116) tends to infinity also for $R \to \infty$, because of the term depending on the hydraulic conductivity. Hence, the right-hand-side has a positive minimum. Numerical simulations showed that the minimum is unique. Recalling the assumed properties of $\psi(R)$, we can conclude that (116) has either one or two solutions or no solutions at all. When two solutions exist, the physical one is the smaller (for a spheroid that has grown to the steady state from a small size). If $\psi(R) \equiv 0$, i.e. for spheroids growing in aqueous suspension, Eq. (116) can only have zero or two solutions. This latter case will be illustrated in the section of the numerical results.

9 Numerical results

All the numerical results refer to the case $\theta_\tau \to 0$. First of all, we illustrate the stationary state by showing the behaviour of Eq. (116). When $\theta_\tau \to 0$, in (116) $\rho_\tau = \rho_N$ and the last term in the r.h.s. vanishes. In the following simulations, the parameters of oxygen consumption have the same values of those given in section 4. As to the mechanical parameters, we chose as reference values $K = 10^{-7}\,\mathrm{cm}^3\cdot\mathrm{s/g}$, $\eta_C = 10^4\,\mathrm{g/(cm\cdot s)}$ and $\nu = 0.6$. For the hydraulic conductivity, values two or three orders of magnitude less have been reported for solid tumours [39]. However, we may observe that the cell number density and the ECM content of *in vivo* tumours are likely to be higher than in the *in vitro* spheroids. The chosen value of cell viscosity was suggested by measurements reported in [32].

Fig. 2, left panel, shows the left and the right-hand-side of (116), whose intersection determines the value of R at the steady state, for $\psi(R) = 0$ and $\gamma = 1\,\text{dyne/cm}$, $\tau_0 = 10\,\text{dyne/cm}^2$. With these parameter values, the necessary condition (61) is satisfied and we have $p_C > p_E$ in stages II and III. The predicted stationary R is $966\,\mu\text{m}$, a value in the experimentally observed range. The plot shows the vertical asymptote for $R = R_a$. For very large R, beyond the range of the figure, the r.h.s. of (116) attains a minimum and then slightly increases. Since the intersection is on the branch approaching the asymptote, the value of ρ_D will be small. Note that, owing to the presence of the asymptote, the stationary R has a very mild dependence on γ in the whole range $\gamma > 0.6\,\text{dyne/cm}$. The right panel of Fig. 2 reports the different terms whose sum gives the r.h.s. of (116).

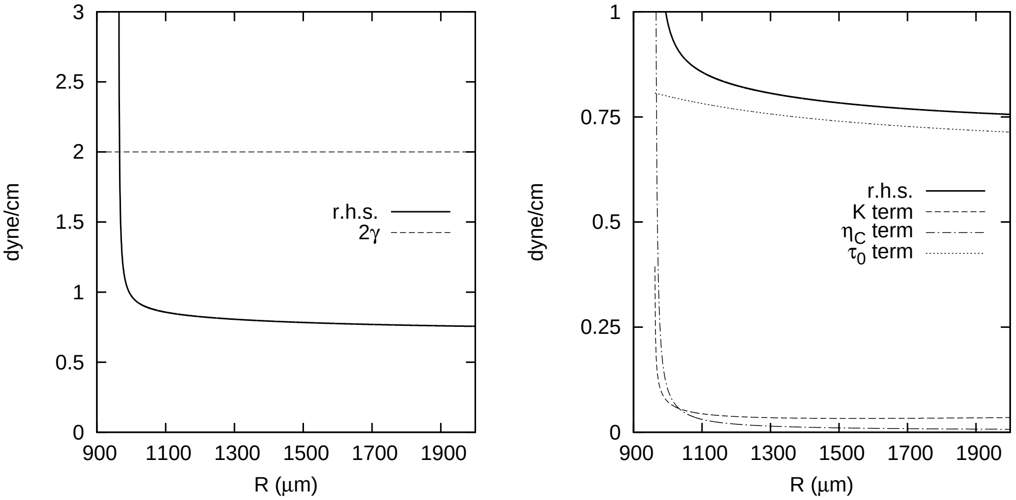

Figure 2: Left panel: Profile of right-hand-side (solid) and left-hand-side (dashed) of (116) as a function of R. Right panel: Plot of the different terms of the right-hand-side of (116). $\gamma = 1\,\text{dyne/cm}$, $\tau_0 = 10\,\text{dyne/cm}^2$. Other parameters indicated in the text. The predicted stationary radius is $R = 966\,\mu\text{m}$.

The time evolution of the spheroid starting from $R(0) = 125\,\mu\text{m}$, with the parameters as above and $\chi = \ln 2/24\,\text{h}^{-1}$, $\theta_D = 48\,\text{h}$ is reported in Fig. 3. Note that the stationary radius (whose value agrees with the prediction given by Eq. (116)) is attained at about 30 days and that the radius of the liquid core is only 1/5 of the radius of the whole necrotic region.

Since the factor multiplying τ_0 in Eq. (116) is positive, for a given value of γ and τ_0 increasing the stationary radius is predicted to increase. However, since both γ and τ_0 are due to the intercellular adhesion bonds, we cannot infer that the stationary radius increases as the number and/or the strength of the intercellular bonds increase.

It is evident from Fig. 2 that, when γ decreases, as long as the constraints ensuring existence are satisfied, the stationary radius increases until no intersection can be found. In this case an unbounded evolution would take place. However, with $\tau_0 = 10\,\text{dyne/cm}^2$ and the reference values of the other parameters, the neces-

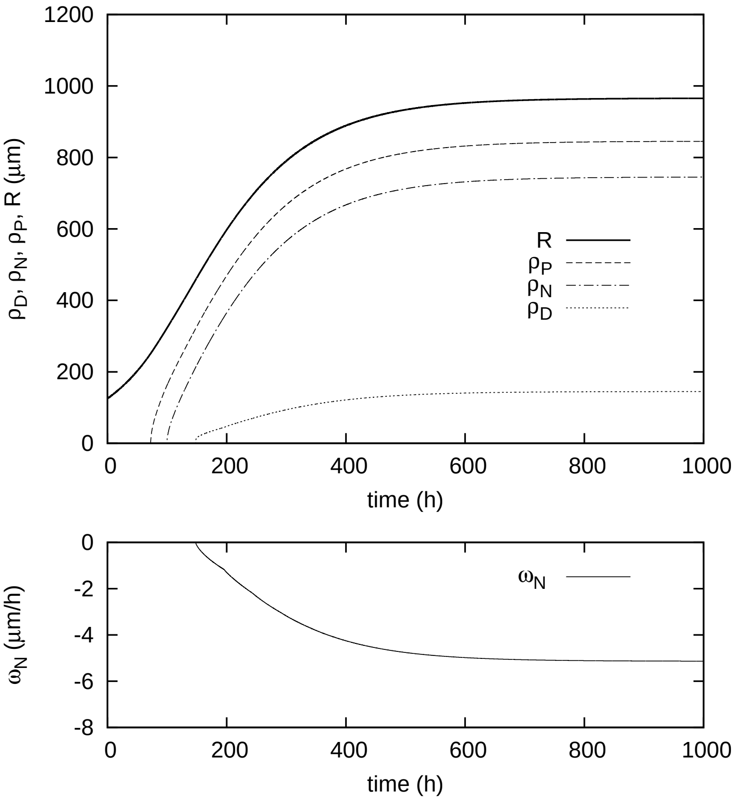

Figure 3: Upper panel: Time evolution of the external radius and of all the interfaces. The velocity ω_N is reported in the lower panel. $\gamma = 1\,\text{dyne/cm}$, $\tau_0 = 10\,\text{dyne/cm}^2$. Other parameters indicated in the text.

sary condition (61) is not satisfied for the values of γ providing no intersection (e.g., $\gamma = 0.25\,\text{dyne/cm}$). By analyzing the region of the (γ, τ_0) plane in which condition (61) is satisfied, a zone can be found where the constraint is satisfied and the evolution is unbounded. In particular, with $K = 10^{-8}\text{cm}^3{\cdot}\text{s/g}$, $\gamma = 0.02\,\text{dyne/cm}$ and $\tau_0 = 0.2\,\text{dyne/cm}^2$, we get the profile of the r.h.s. of (116) shown in Fig. 4 and the time evolution shown in Fig. 5. In this case, the velocity ω_N was found to be rather small in absolute value.

Experimental measurements of the rupture force of a single cadherin-cadherin bond – cadherins are the main family of cell membrane molecules mediating cell adhesion – indicate a mean value of 30 pN for N-cadherins (70 pN for E-cadherins) [40] (see also [5]). A crude estimation of the yield stress in a cell aggregate can be given by $\tau_0 = Fn^{2/3}$, where F is the force needed to detach two adhering cells and n is the cell number density. According to the above estimate and setting n to the value of $2.8 \cdot 10^8$ cells/cm^3 [26], the contribution to yield stress by a single N-cadherin bond is $1.29\,\text{dyne/cm}^2$. As multiple bonds are likely to be involved in cell adhesion, small values of τ_0 (and γ) as in Figs. 4 and 5 appear to be not physical. Therefore,

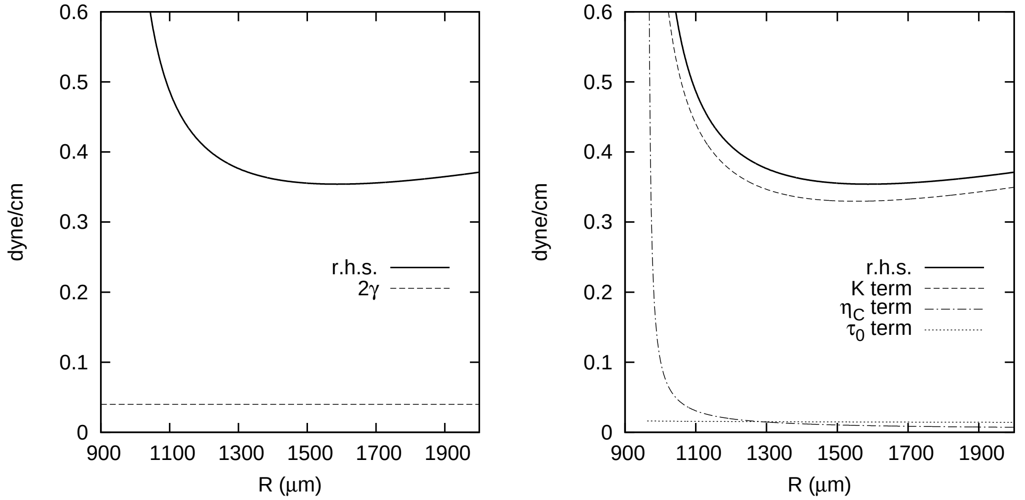

Figure 4: Left panel: Profile of right-hand-side (solid) and left-hand-side (dashed) of (116) as a function of R. Right panel: Plot of the different terms of the right-hand-side of (116). $\gamma = 0.02\,\mathrm{dyne/cm}$, $\tau_0 = 0.2\,\mathrm{dyne/cm}^2$, $K = 10^{-8}\mathrm{cm}^3{\cdot}\mathrm{s/g}$. Other parameters indicated in the text.

although the model in principle allows either evolutions toward the steady state and unbounded evolutions, only the former seem to be permitted with physically reasonable parameter values.

10 Concluding remarks

The present model, based on a two-fluid approach in which the cell component is represented by a Bingham-like fluid and on the assumption that a finite delay is required for degradation of dead cells to liquid, predicts two possible spheroid behaviours: the evolution toward the steady state or an unbounded growth, depending on the values of the mechanical parameters (mainly on the surface tension and the yield stress). This result parallels the prediction of the model proposed by Landman and Please [33]. However, our numerical results suggest that, with reasonable values of the parameters, only the attainment of the steady state is possible.

It is absolutely obvious that most of the assumptions we have made are questionable from the biological point of view under many respects and, moreover, they do not have all the same importance. A critical point is that biological processes that are essentially stochastic are given a deterministic description. The general strategy which was pursued in the present paper was not to deal with each detail of the enormously complex biological structure, but rather to synthesize from it some lean schematic picture, still retaining the principal biological information but playing with the least possible number of parameters.

The presence of interfaces in the model is of course a quite arbitrary approxima-

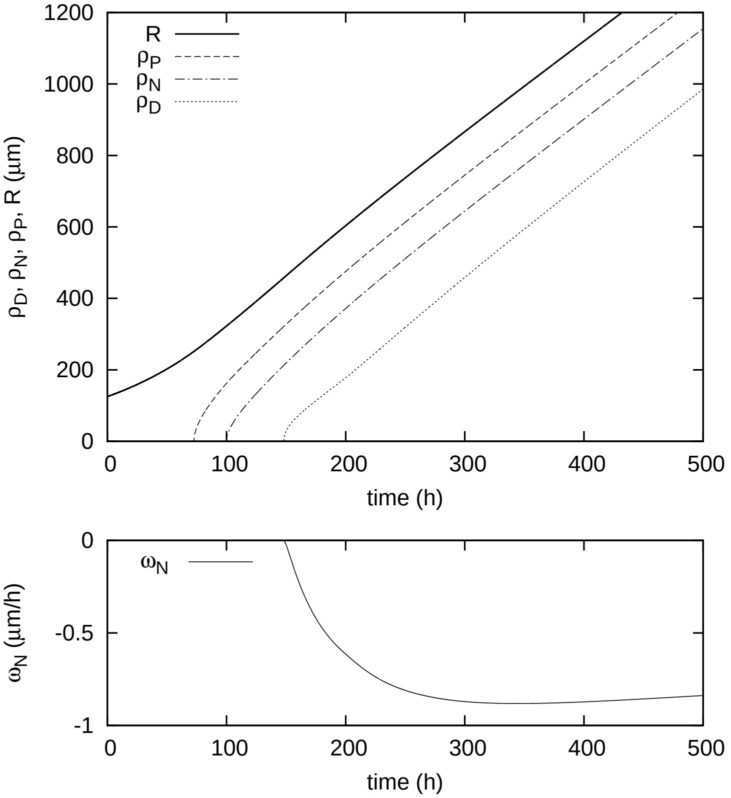

Figure 5: Upper panel: Time evolution of the external radius and of all the interfaces. The velocity ω_N is reported in the lower panel. $\gamma = 0.02\,\text{dyne/cm}$, $\tau_0 = 0.2\,\text{dyne/cm}^2$, $K = 10^{-8}\text{cm}^3{\cdot}\text{s/g}$. Other parameters indicated in the text.

tion, but we do not expect that it may greatly influence the qualitative behaviour of the system. It complicates the numerical calculation (and the mathematical structure), but it represents an advantageous conceptual simplification, providing a neat compartmental partition of the spheroid and allowing in some cases the explicit computation of the velocity fields. Besides performing numerical simulations, emphasizing the important influence of the physical parameters, we have carried out a rigorous analysis of the differential system, obtaining existence and uniqueness results.

The model could be extended in various directions, for instance including glucose metabolism and related effects of acidity. Perhaps the most important extension would be to include the inhibition of proliferation caused by a mutual compression among cells beyond some threshold. This aspect might be integrated in the model by making the proliferation rate dependent on the pressure of the cell fluid. The mathematical analysis, however, would result remarkably more complicated. The interface between proliferating and quiescent cells might, indeed, become dependent on the mechanics instead of being simply dependent on the oxygen diffusion-consumption process.

Acknowledgments

The present work was partially supported by the MIUR-PRIN 2008: "Modelli matematici per sistemi a molte componenti nelle scienze mediche e ambientali".

Appendix

With the aim of computing $p_C(\rho_D^+, t)$ during stage IV, we recall that in each of the intervals (ρ_P, R), (ρ_N, ρ_P) and (ρ_D, ρ_N), $\nabla \cdot \mathbf{u}$ is constant and then the momentum balance equation (17) becomes

$$-p'_C + u'\Big(\frac{\tilde{\tau}_0}{\sqrt{II_D}}\Big)' - \frac{u}{\nu K} = 0\,. \tag{A.1}$$

At the interfaces $r = \rho_P$ and $r = \rho_N$, we impose the continuity of the normal stress. Then, in view of the continuity of p_E, at $r = \rho_P$ we must have

$$\begin{aligned} &-\Big(p_C(\rho_P^+, t) + \frac{2}{3}\eta_C\chi\Big) + \Big(2\eta_C + \frac{\tau_0}{\sqrt{II_D}}\Big)\Big|_{r=\rho_P^+} u'(\rho_P^+, t) \\ &= -p_C(\rho_P^-, t) + \Big(2\eta_C + \frac{\tau_0}{\sqrt{II_D}}\Big)\Big|_{r=\rho_P^-} u'(\rho_P^-, t)\,, \end{aligned}$$

from which we obtain

$$[p_C]_{\rho_P} = \frac{4}{3}\eta_C\chi + \tau_0\left[\left(\frac{1}{\sqrt{II_D(\rho_P^+, t)}} - \frac{1}{\sqrt{II_D(\rho_P^-, t)}}\right)u'(\rho_P^-, t) + \frac{\chi}{\sqrt{II_D(\rho_P^+, t)}}\right], \tag{A.2}$$

where $[p_C]_{\rho_P} = p_C(\rho_P^+, t) - p_C(\rho_P^-, t)$. At $r = \rho_N$, instead, since $\nabla \cdot \mathbf{u}$, u', II_D, and $\tilde{\tau}_0$ are continuous (together with p_E) with respect to r, the cell pressure p_C is continuous. When $\theta_\tau < \theta_D$, the same continuity holds at the boundary $r = \rho_\tau$.

Thus, integrating (A.1) from ρ_D to R and taking into account the jump $[p_C]_{\rho_P}$, we get

$$p_C(\rho_D^+, t) = p_C(R, t) - [p_C]_{\rho_P} - \int_{\rho_\tau}^{\rho_N} u'\Big(\frac{\tilde{\tau}_0}{\sqrt{II_D}}\Big)' dr - \tau_0 \int_{\rho_N}^{R} u'\Big(\frac{1}{\sqrt{II_D}}\Big)' dr + \int_{\rho_D}^{R} \frac{u}{\nu K}\, dr\,, \tag{A.3}$$

where, in the last two integrals of (A.3), the velocity u and the invariant II_D are intended to have different expressions in the regions P and Q ∪ NS.

Taking into account (A.3), and that

$$p_E(\rho_D, t) = p_{ext} - \int_{\rho_D}^{R} \frac{u}{(1-\nu)K}\, dr,$$

Eq. (52) can be rewritten as:

$$p_C(R,t) - p_{ext} - [p_C]_{\rho_P} - \int_{\rho_\tau}^{\rho_N} u'\Big(\frac{\tilde{\tau}_0}{\sqrt{II_D}}\Big)'\, dr - \tau_0 \int_{\rho_N}^{\rho_P} u'\Big(\frac{1}{\sqrt{II_D}}\Big)'\, dr$$
$$-\tau_0 \int_{\rho_P}^{R} u'\Big(\frac{1}{\sqrt{II_D}}\Big)'\, dr + \int_{\rho_D}^{R} \frac{u}{\nu(1-\nu)K}\, dr - 2\eta_C u'(\rho_D^+,t) \; = 0. \tag{A.4}$$

By performing the integration by parts

$$\int_{r_1}^{r_2} u'\big(\frac{1}{\sqrt{II_D}}\big)'\, ds = u'\frac{1}{\sqrt{II_D}}\Big|_{r_1}^{r_2} - \int_{r_1}^{r_2} \frac{u''}{\sqrt{II_D}}\, ds\,,$$

and recalling (23) and (A.2), Eq. (A.4) reduces to

$$\frac{2\gamma}{R} + \psi(R) - 2\eta_C\chi + 2\eta_C\big(u'(R,t) - u'(\rho_D,t)\big) - \int_{\rho_\tau}^{\rho_N} u'\Big(\frac{\tilde{\tau}_0}{\sqrt{II_D}}\Big)'\, dr$$
$$+\tau_0 \int_{\rho_N}^{\rho_P} \frac{u''}{\sqrt{II_D}}\, dr + \tau_0 \int_{\rho_P}^{R} \frac{u''}{\sqrt{II_D}}\, dr + \int_{\rho_D}^{R} \frac{u}{\nu(1-\nu)K}\, dr - 2\eta_C u'(\rho_D^+,t) \; = 0. \tag{A.5}$$

Recalling (49) and integrating by parts we have

$$\int_{\rho_\tau}^{\rho_N} u'\Big(\frac{\tilde{\tau}_0}{\sqrt{II_D}}\Big)'\, dr = \tau_0\, \frac{1 - \frac{\theta(r,t)}{\theta_\tau}}{\sqrt{II_D}} u'\Bigg|_{\rho_\tau}^{\rho_N} - \tau_0 \int_{\rho_\tau}^{\rho_N} \frac{u''}{\sqrt{II_D}}\, dr + \frac{\tau_0}{\theta_\tau}\int_{\rho_\tau}^{\rho_N} \frac{\theta(r,t)}{\sqrt{II_D}}\, dr\,.$$

Since $\theta(\rho_N,t) = 0$, $\theta(\rho_\tau,t) = \theta_\tau$, and $u = \rho_N^2\omega_N/r^2$, $\sqrt{II_D} = \sqrt{3}\rho_N^2|\omega_N|/r^3$, we obtain

$$\int_{\rho_\tau}^{\rho_N} u'\Big(\frac{\tilde{\tau}_0}{\sqrt{II_D}}\Big)'\, dr = -\frac{2}{\sqrt{3}}\tau_0 \mathrm{sgn}(\omega_N) - 2\sqrt{3}\tau_0 \mathrm{sgn}(\omega_N) \ln\frac{\rho_N}{\rho_\tau}$$
$$+ 2\sqrt{3}\frac{\tau_0}{\theta_\tau}\mathrm{sgn}(\omega_N)\int_{\rho_\tau}^{\rho_N} \frac{\theta(r,t)}{r}\, dr\,. \tag{A.6}$$

Similarly we obtain

$$\int_{\rho_N}^{\rho_P} \frac{u''}{\sqrt{II_D}}\, dr = 2\sqrt{3}\mathrm{sgn}(\omega_N) \ln\frac{\rho_P}{\rho_N}\,. \tag{A.7}$$

In region P, in view of (46), we have instead

$$u'' = \frac{6}{r^4}(\rho_N^2\omega_N - \frac{\chi}{3}\rho_P^3)\,,$$

$$II_D = \big(\frac{\chi^2}{3}\rho_P^6 - 2\chi\rho_N^2\omega_N\rho_P^3 + 3\rho_N^4\omega_N^2\big)\frac{1}{r^6} + \frac{\chi^2}{6}\,,$$

and then we can write

$$\int_{\rho_P}^{R} \frac{u''}{\sqrt{II_D}}\, dr = \sqrt{2}\chi A \int_{\rho_P}^{R} \frac{1}{\sqrt{\frac{\chi^2}{6}\big(1 + \frac{A^2}{r^6}\big)}}\frac{1}{r^4}\, dr\,,$$

where

$$A = \frac{\sqrt{6}}{\chi}(\sqrt{3}\rho_N^2\omega_N - \frac{\chi}{\sqrt{3}}\rho_P^3). \tag{A.8}$$

By setting $z = 1/r^3$, the above integral becomes

$$\frac{2}{\sqrt{3}}A\int_{1/R^3}^{1/\rho_P^3} \frac{dz}{\sqrt{1+A^2z^2}}\,,$$

and, setting also $|A|z = \sinh(\xi)$, we get

$$\int_{\rho_P}^{R} \frac{u''}{\sqrt{II_D}}\,dr = \frac{2}{\sqrt{3}}\frac{A}{|A|}\ln\frac{\frac{1}{\rho_P^3}+\sqrt{\frac{1}{A^2}+\frac{1}{\rho_P^6}}}{\frac{1}{R^3}+\sqrt{\frac{1}{A^2}+\frac{1}{R^6}}}\,. \tag{A.9}$$

Moreover, taking into account (45) and (46), we have

$$\int_{\rho_D}^{R} \frac{u}{\nu(1-\nu)K}\,dr = \frac{1}{\nu(1-\nu)K}\Big\{\rho_N^2\omega_N\Big(\frac{1}{\rho_D}-\frac{1}{R}\Big) + \frac{\chi}{3}(R-\rho_P)^2\Big(\frac{1}{2}+\frac{\rho_P}{R}\Big)\Big\}\,. \tag{A.10}$$

Finally, from Eqs. (A.6), (A.7), (A.8), (A.9) and (A.10), and expressing $u'(R,t)$, $u'(\rho_D^+,t)$ by means of (46), (45), Eq. (A.5) can be written as follows:

$$\begin{aligned}
\frac{2\gamma}{R} &= -\psi(R) + 4\eta_C\rho_N^2\omega_N\Big(\frac{1}{R^3}-\frac{1}{\rho_D^3}\Big) + \frac{4}{3}\eta_C\chi\Big[1-\Big(\frac{\rho_P}{R}\Big)^3\Big] \\
&- \frac{1}{\nu(1-\nu)K}\Big\{\rho_N^2\omega_N\Big(\frac{1}{\rho_D}-\frac{1}{R}\Big) + \frac{\chi}{3}(R-\rho_P)^2\Big(\frac{1}{2}+\frac{\rho_P}{R}\Big)\Big\} \\
&+ 2\sqrt{3}\tau_0\Bigg[-\mathrm{sgn}(\omega_N)\ln\frac{\rho_P}{\rho_\tau} - \frac{1}{3}\mathrm{sgn}\Big(\sqrt{3}\rho_N^2\omega_N - \frac{\chi}{\sqrt{3}}\rho_P^3\Big) \\
&\times \ln\frac{\Big(\frac{R}{\rho_P}\Big)^3 + \sqrt{\frac{\chi^2R^6}{6\big(\frac{\chi}{\sqrt{3}}\rho_P^3-\sqrt{3}\rho_N^2\omega_N\big)^2}+\Big(\frac{R}{\rho_P}\Big)^6}}{1+\sqrt{\frac{\chi^2R^6}{6\big(\frac{\chi}{\sqrt{3}}\rho_P^3-\sqrt{3}\rho_N^2\omega_N\big)^2}+1}} + \frac{1}{\theta_\tau}\mathrm{sgn}(\omega_N)\int_{\rho_\tau}^{\rho_N}\frac{\theta(r,t)}{r}\,dr\Bigg]\,.
\end{aligned} \tag{A.11}$$

By imposing $\omega_N < 0$, (A.11) reduces to (53).

Let us consider now the special case $\theta_\tau = 0$, in which $\tilde{\tau}_0 = 0$ for $\rho_D < r < \rho_N$ and the whole region NS behaves as a Newtonian fluid. At $r = \rho_N$, the continuity of the normal stress writes as

$$-p_C(\rho_N^+,t) + \left(2\eta_C + \frac{\tau_0}{\sqrt{II_D}}\right)\Bigg|_{r=\rho_N^+} u'(\rho_N^+,t) = -p_C(\rho_N^-,t) + 2\eta_C u'(\rho_N^-,t)\,,$$

from which we obtain

$$[p_C]|_{r=\rho_N} = \frac{\tau_0}{\sqrt{II_D}}\bigg|_{r=\rho_N^+} u'(\rho_N^+, t) = -\frac{2}{\sqrt{3}}\tau_0 \mathrm{sgn}(\omega_N)\,,$$

where $[p_C]|_{r=\rho_N} = p_C(\rho_N^+, t) - p_C(\rho_N^-, t)$. By integrating (A.1) we then have

$$p_C(\rho_D^+, t) = p_C(R, t) - [p_C]_{\rho_P} - [p_C]_{\rho_N} - \tau_0 \int_{\rho_N}^{R} u' \Big(\frac{1}{\sqrt{II_D}}\Big)' \, dr + \int_{\rho_D}^{R} \frac{u}{\nu K} \, dr\,,$$

and, proceeding as above, we still get Eq. (56) after assuming $\omega_N < 0$. Substantially, this result relies on the fact that the limit of (A.6) for $\theta_\tau \to 0$ is exactly equal to $[p_C]_{\rho_N}$ as given by Eq. (10).

References

[1] J.A. Adam and S.A. Maggelakis. Diffusion regulated growth characteristics of a spherical prevascular carcinoma. *Bull. Math. Biol.*, 52:549–582, 1990.

[2] D. Ambrosi and L. Preziosi. Cell adhesion mechanisms and stress relaxation in the mechanics of tumours. *Biomech. Model. MechanoBiol.*, 8:397–413, 2009.

[3] R.P. Araujo and D.L.S. McElwain. A history of the study of solid tumour growth: the contribution of mathematical modelling. *Bull. Math. Biol.*, 66:1039–1091, 2004.

[4] I.V. Basov and V.V. Shelukhin. Generalized solutions to the equations of compressible bingham flows. *Z. Angew. Math. Mech.*, 79:185–192, 1999.

[5] W. Baumgartner, Hinterdorfer P., W. Ness, A. Raab, D. Vestweber, H. Schindler, and D. Drenckhahn. Cadherin interaction probed by atomic force microscopy. *Proc. Natl. Acad. Sci. USA*, 97:4005–4010, 2000.

[6] N. Bellomo, N.K. Li, and P.K. Maini. On the foundations of cancer modelling: selected topics, speculations, and perspectives. *Math. Mod. Meth. Appl. Sci.*, 18:593–646, 2008.

[7] A. Bertuzzi, C. Bruni, A. Fasano, A. Gandolfi, F. Papa, and C. Sinisgalli. Response of tumor spheroids to radiation: Modeling and parameter identification. *Bull. Math. Biol.*, 72:1069–1091, 2010.

[8] A. Bertuzzi, A. Fasano, and A. Gandolfi. A free boundary problem with unilateral constraints describing the evolution of a tumour cord under the influence of cell killing agents. *SIAM J. Math. Anal.*, 36:882–915, 2004.

[9] A. Bertuzzi, A. Fasano, and A. Gandolfi. A mathematical model for tumor cords incorporating the flow of interstitial fluid. *Math. Mod. Meth. Appl. Sci.*, 15:1735–1777, 2005.

[10] A. Bertuzzi, A. Fasano, A. Gandolfi, and C. Sinisgalli. ATP production and necrosis formation in a tumour spheroid model. *Math. Model. Nat. Phenom.*, 2:30–46, 2007.

[11] A. Bertuzzi, A. Fasano, A. Gandolfi, and C. Sinisgalli. Necrotic core in EMT6/Ro tumor spheroids: Is it caused by an ATP deficit? *J. Theor. Biol.*, 262, 2010.

[12] L. Bianchini and A. Fasano. A model combining acid-mediated tumour invasion and nutrient dynamics. *Nonlin. Anal. Real World Appl.*, 10, 2009.

[13] A. Bredel-Geissler, U. Karbach, S. Walenta, L. Vollrath, and W. Mueller-Klieser. Proliferation-associated oxygen consumption and morphology of tumour cells in monolayer and spheroid culture. *J. Cell. Physiol.*, 153:44–52, 1992.

[14] C.J. Breward, H.M Byrne, and C.E. Lewis. The role of cell-cell interactions in a two-phase model for avascular tumour growth. *J. Math. Biol.*, 45:125–152, 2002.

[15] H.M Byrne and M.A.J. Chaplain. Growth of necrotic tumors in the presence and absence of inhibitors. *Math. Biosci.*, 135:187–216, 1996.

[16] H.M Byrne, J.R. King, D.L.S. McElwain, and Preziosi L. A two-phase model of solid tumour growth. *Appl. Math. Lett.*, 16:567–573, 2003.

[17] H.M. Byrne and L. Preziosi. Modelling solid tumour growth using the theory of mixtures. *Math. Med. Biol.*, 20:341–366, 2003.

[18] J.J. Casciari, S.V. Sotirchos, and R.M. Sutherland. Mathematical modelling of microenvironment and growth in EMT6/Ro multicellular tumour spheroids. *Cell Prolif.*, 25:1–22, 1992.

[19] S. Cui and A. Friedman. Analysis of a mathematical model of the growth of necrotic tumors. *J. Math. Anal. Appl.*, 255:636–677, 2001.

[20] A. Fasano, M. Gabrielli, and A. Gandolfi. Investigating the steady state of multicellular spheroids by revisiting the two-fluid model. *Math. Biosci. Eng.*, 8:239–252, 2011.

[21] A. Fasano, M. Gabrielli, and A. Gandolfi. Erratum to: Investigating the steady state of multicellular spheroids by revisiting the two-fluid model. *Math. Biosci. Eng.*, 9:697, 2012.

[22] A. Fasano and A. Gandolfi. The steady state of multicellular tumour spheroids: a modelling challenge. In U. Ledzewicz, H. Schaettler, A. Friedman, and E. Kashdan, editors, *Mathematical Methods and Models in Biomedicine*, pages 161–179. Springer, New York, 2012.

[23] A. Fasano, A. Gandolfi, and M. Gabrielli. The energy balance in stationary multicellular spheroids. *Far East J. Math. Sci.*, 39:105–128, 2010.

[24] J. Folkman and M. Hochberg. Cell-regulation of growth in three dimensions. *J. Exp. Med.*, 138, 1973.

[25] J.P. Freyer and R.M. Sutherland. A reduction in the in situ rates of oxygen and glucose consumption of cells in EMT6/Ro spheroids during growth. *J. Cell. Physiol.*, 124:516–524, 1985.

[26] J.P. Freyer and R.M. Sutherland. Regulation of growth saturation and development of necrosis in EMT6/Ro multicellular spheroids by the glucose and oxygen supply. *Cancer Res.*, 46:3504–3512, 1986.

[27] A. Friedman. A hierarchy of cancer models and their mathematical challenges. *Discr. Cont. Dyn. Syst. B*, 4:147–159, 2004.

[28] P. Greenspan. Models for the growth of a solid tumour by diffusion. *Stud. Appl. Math.*, 51:317–340, 1972.

[29] G. Hamilton. Multicellular spheroids as an in vitro tumor model. *Cancer Lett.*, 131:29–34, 1998.

[30] G. Helmlingen, P.A. Netti, H.C. Lichtembeld, R.J. Melder, and R.K. Jain. Solid stress inhibits the growth of multicellular tumor spheroids. *Nature Biotech.*, 15:778–783, 1997.

[31] J. Humphrey and K. Rajagopal. A constrained mixture model for growth and remodeling of soft tissues. *Math. Mod. Meth. Appl. Sci.*, 22:407–430, 2002.

[32] A. Iordan, A. Duperray, and Verdier C. A fractal approach to the rheology of concentrated cell suspensions. *Phis. Rev. E*, 77:011911, 2008.

[33] K.A. Landman and C.P. Please. Tumour dynamics and necrosis: surface tension and stability. *IMA J. Math. Appl. Med. Biol.*, 18:131–158, 2001.

[34] J.S. Lowengrub, H.B. Frieboes, F. Jin, Y.L. Chuang, X. Li, P. Macklin, S.M. Wise, and Cristini. V. Nonlinear modelling of cancer: bridging the gap between cells and tumours. *Nonlinearity*, 23:1–91, 2010.

[35] W. Mueller-Klieser. Method for the determination of oxygen consumption rates and diffusion coefficients in multicellular spheroids. *Biophys. J.*, 46:343–348, 1984.

[36] W. Mueller-Klieser. Three dimensional cell cultures: from molecular mechanisms to clinical applications. *Am. J. Physiol.*, 273:C1109–C1123, 1997.

[37] W. Mueller-Klieser. Tumor biology and experimental therapeutics. *Crit. Rev. Hematol. Oncol.*, 36:123–139, 2000.

[38] M. Neeman, K.A. Jarrett, L.O. Sillerud, and J.P. Freyer. Self-diffusion of water in multicellular spheroids measured by magnetic resonance microimaging. *Cancer Res.*, 51:4072–4079, 1991.

[39] P.A. Netti and R.K. Jain. Interstitial transport in solid tumours. In L. Preziosi, editor, *Cancer Modelling and Simulation*, pages 51–74. Chapman&Hall/CRC, Boca Raton, 2003.

[40] P. Panorchan, M.S. Thompson, K.J. Davis, Y. Tseng, K. Konstantopoulos, and D. Wirtz. Single-molecule analysis of cadherin-mediated cell-cell adhesion. *J. Cell Sci.*, 119:66–74, 2006.

[41] L. Preziosi and G. Vitale. A multiphase model of tumor and tissue growth including cell adhesion and plastic reorganization. *Math. Mod. Meth. Appl. Sci.*, 21:1901–1932, 2011.

[42] K.R. Rajagopal and L. Tao. *Mechanics of Mixtures*. World Scientific, Singapore, 1995.

[43] I. Rao, J. Humphrey, and K. Rajagopal. Biological growth and remodeling: a uniaxial example with possible application to tendons and ligaments. *Comp. Mod. Engrg. Sci.*, 4:439–495, 2003.

[44] K. Smallbone, R.A. Gatenby, R.J. Gillies, P.K. Maini, and D.J. Gavaghan. Metabolic changes during carcinogenesis: potential impact on invasiveness. *J. Theor. Biol.*, 244:703–713, 2007.

[45] K. Smallbone, D.J. Gavaghan, R.A. Gatenby, and P.K. Maini. The role of acidity in solid tumour growth and invasion. *J. Theor. Biol.*, 235:476–484, 2005.

[46] R.M. Sutherland. Cell and environment interactions in tumor microregions: the multicell spheroid model. *Science*, 240:177–184, 1988.

[47] R. Venkatasubramanian, M.A. Henson, and N.S. Forbes. Incorporating energy metabolism into a growth model of multicellular tumor spheroids. *J. Theor. Biol.*, 242:440–453, 2006.